Reply to Editor

Dear Editor,

as you recognized in your initial decision letter, we already changed the paper one time according to the comments of reviewer # 1 an three times according to the comments of reviewer #2. On the basis of your indication, we further modified the paper to meet the requirements of reviewer #1 " to make a link with another domain in Earth sciences which would make this paper more interesting for HESS readers" and of reviewer #2 " to clearly indicate the objectives of the study and the domain of applications by modifying the title, the objectives and the related sections in the paper".

In the previous replies we didn't do that because we are not fully convinced that to expand the discussion, in view also of a limitation of the paper size, can really help the reader to better understand the potentialities of the proposed methodology. In the revised version, we first changed the focus of the paper (and also its title) from the simple discharge computation to the computation of the averaged vertical velocities along a river cross-section. We showed why this is a central issue for the reliability of the flow routing models and, in the conclusions, also for the computation of the bed load transport in irregular sections, as required by reviewer #1.

Unfortunately, there are not field data in literature accurate enough to expand the validation of our model also to the prediction of solid transport data, as we did for the discharge. The reason is that all transport formulas compute values per unit width and solid transport experiments are carried out on flumes with large rectangular section.

In the reply to reviewers we enclose, for their convenience, the previous comments and the corresponding replies, as well as a comment on the changes made on the basis of your indications. We also enclose, along with a copy of the paper changed according with all the previous comments and replies, a copy of the finally submitted paper, where the changes with respect to the previous one are underlined.

Computation of vertically averaged velocities in irregular sections of straight channels

Reply to review of J.B. Faure (reviewer #1)

Previous review and reply

We first thank the reviewer for his valuable job.

General Comments:

Point 1: *The paper is out of the scope of HESS.*

Reply: We don't agree with the reviewer for the following (see http://www.hydrology-and-earth-system-sciences.net/about/aims_and_scope.html): a) among the others, the scope of HESS encompasses the following:

2. **the study of the spatial and temporal characteristics of the global water resources** (solid, **liquid**, and vapour) and related budgets, in all compartments of the Earth system (atmosphere, oceans, estuaries, **rivers**, lakes, and land masses), including water stocks, residence times, interfacial fluxes, and the pathways between various compartments;

b) among the others, the journal covers the following subject areas and techniques/approaches, which are used to categorize papers:

Subject areas:

1. **rivers** and lakes;
2. **engineering hydrology**;
3. **water resources management**.

c) among the others, the following techniques and approaches:

- **modelling approaches;**
- instruments and **observation techniques;**
- **uncertainty analysis.**

Point 2: *the paper is a pure hydraulics/fluid mechanics paper*

Reply: we don't agree with the reviewer because both formulas are not based on advanced integration of the Reynolds equations, but are founded on the historical experience of the Manning formula and on three different validation tests carried out on the basis of laboratory and field data, as well as of the results of 3D numerical analysis (carried out with a commercial code). In the introduction, we have shown that integration of the Reynolds equations leads to formulas that depend on several empirical coefficients. On the basis of the previous observation, we go on with a different approach, strongly based on experimental evidence.

Point 3: *is it a bad idea….*?

We agree with the reviewer about the possibility of using the developed approach to simply estimate the vertically averaged velocity in single sub-sections and use this velocity value for the 1D transport equation in the same sub-

section. On the other hand, we think that a preliminary requirement is to have some evidence that the proposed approach provides reliable results before using it for this and other possible applications.
The focus of our paper is about this evidence.

Questions:

Question 1): *When they are used in 1D shallow water simulations, the purpose of this kind of head loss formulas is to take into account the lateral variation of the roughness / flow resistance, that is, in fact, the Manning coefficient. In the paper only a constant Manning coefficient is considered. Even when the formulas are validated against a real case, the Manning coefficient is taken constant along a river reach 13 km long. I am pretty sure that it is possible to obtain the same agreement with standard calibration of Manning-Strickler formula and a Manning coefficient different in several sub-reaches.*

Reply: We first want to say that we don't fully agree with the remark in the premises of the question. This type of formulas is not motivated by the lateral variation of the roughness, but by the effect of the geometrical irregularity of the section. All the empirical formulas, like the Manning formula, are based on experiments carried out on sections with convex shapes (triangular, rectangular, trapezoidal or circular) and do not take into account the lateral variability of the vertically averaged velocity.
The lateral variability of the Manning coefficient is another source of uncertainty. With the proposed approach, we can easily differentiate the Manning coefficient along the section. Results will be reliable assuming that the secondary effect of the Manning coefficient lateral variation does not affect the relative dependency of the velocities, as structured in the homogeneous case.
The comment relative to the validation test number 2) does not take into account that the Manning coefficient has, in the context of the indirect method for discharge estimation, the meaning of a calibration parameter, that we use to match the water levels measured in the downstream section with the level computed by the 1D hydraulic model.
It is well known from the parameter estimation theory (*Aster et al., 2012*) that in any numerical model the uncertainty of the estimated parameters, obtained by matching the computed and the measured model output, grows very quickly with the parameter number. This implies the need of minimizing the number of parameters, also by neglecting the effect of irregularities and heterogeneities. Of course, it would be very easy to fit very well the measured and the computed water level hydrographs (that are the output of the hydraulic model) also by differentiating the Manning coefficient along the reach or along the section, but the corresponding parameter error would become very large even with a small error in the topography or in the measured water levels. These errors strongly affect the discharge computed by the hydraulic model. Moreover, if the computed Manning coefficients or the parameters of other formulas were used for prediction purpose (which is a major benefit of the indirect measurement approach) the predicted discharges would be affected by an even stronger error. All this implies, of course, that test n.2 can be thought as the validation of the proposed formulas for their use in the specific method for the discharge estimation.
On the other hand, as explained in the paper, it is very difficult to carry on field tests for the validation of these formulas, because roughness coefficients are unknown and the results of all formulas can be scaled according to the selected Manning coefficient or to other parameters. The indirect method provides a unique possibility of carrying on a simultaneous estimation of both the Manning coefficient and the discharge hydrograph.
In the revised paper we expanded the introduction to the indirect discharge measurement method by adding:
" It is well-known in the parameter estimation theory (Aster et al., 2012) that the uncertainty of the estimated parameters (in our case the roughness coefficient) grows quickly with the number of parameters, even if the matching between the measured and the estimated model variables (in our case the water stages in the downstream section) improves. The use of only one single parameter over all the computational domain is motivated by the need of getting a robust estimation of the Manning's coefficient and of the corresponding discharge hydrograph."

Question 2): *It would have been interesting to compare the formulas against a standard 2D shallow water simulation, in both cases laboratory flume and real river.*

Reply: It is easy to show that to solve on the river domain a standard 2D finite volume model where turbulence inter-element strains are neglected is equivalent to implement the DCM method in a 1D model where the distance between two sections is similar to the longitudinal extension of the 2D elements and the width of each subsection is similar to the lateral extension of the 2D elements. It would be possible to apply the same strategy implemented in the 1D case also in the 2D case, in order to approximate the inter-element strains without the need of solving complex 2D turbulence models. Once again (see reply do points 2 and 3 of general comments) we preferred to maintain the focus of the paper on the validation of the proposed formulas, even if several application and extensions can be easily foreseen (which we believe is a positive indicator).

Question 3): *equation 1: if I understand the paragraph following this equation well, the energy slope is assumed to be identical in each sub-section, so the subscript for S_f is erroneous*

Reply: We corrected the mistake

Question 4): *page 2618, line 10: "If β is close to zero, …". This point is not clear for me; LRHM appears, at this point, like a continuous formula when DCM is a discrete formula.*

Reply: In Eq. (17a) the limit of the local radius at the l.h.s. for $\beta \to 0$ is equal to *h*. This implies that, in this case, velocity *U* computed in Eq. (16) is independent from the other velocities, as in the DCM approach. DCM can be thought as a spatial discretization of Eq. (15), where the local radius is replaced by *h*, in the same way the practical solution of the LRHM method is obtained by numerical integration of its continuous form given by Eqs. (15)-(17), with β different from zero. We changed the paragraph according to:
"After numerical discretization, Eqs (15)-(17) can be solved to get the unknown q, as well as the vertically averaged velocities in each subsection. If β is close to zero and the size of each subsection is common for both formulas, LHRM is equivalent to DCM; if β is very large LHRM is equivalent to the traditional Manning formula."

Question 5): *page 2619, last line: the numbering scheme of the validations look like a typo.*

Reply: We corrected the mistake

Question 6): *page 2620, §3.4: How is Δq computed?*

Reply: ΔQ is the difference between the discharges computed using two different β values. In the revised paper we specified the meaning of the symbols and also gave the size of the perturbation Δβ used in the sensitivity analysis ($\Delta\beta = 0.001\,\beta$).

Question 7): *page 2622, point 2 (lines 4-5): this (widely used) statement needs a discussion. It is surprising that it is said that the Manning coefficient is varying with the water depth, and not that it is the exponent in the relationship expressing Chezy coefficient in terms of Manning coefficient and hydraulic radius, or that the whole relationship should be revisited. Why the Manning coefficient and not the other terms of the formula?*

Reply: We partially agree with the reviewer. The historical lab experiences that are the basis of the Manning coefficient (set back in time much further than the referenced paper of Herschel of 1897) have been carried out with sections of simple geometry and, of course, with very simple measurement devices. On the other hand, it is common opinion that the roughness of the river bed is strictly related to the size of its irregularities, relative to the actual water depth. If the water depth is small even small grains have a significant relative size, but during flood only the main vegetation has a significant relative size. In parts of the river bed that are commonly submerged by water the same water provides a smoothing of the natural irregularities, but in the other parts submerged only during floods the water flow is likely to get a larger resistance.

Question 8) *page 2623, lines 21-22: it seems that there is a missing word (verb) in this statement.*

Reply: Right. It should be: 'The error obtained between measured and computed discharges, with all methods, **is** of the same order of the discharge measurement error."

Question 9) *page 2627, lines 8-10: that does not prove that an uniform flow has been reached. For that, the same condition must be verified in each cross section along the reach, so that the energy slope equals the bottom slope.*

Reply: Uniform flow conditions do not exist in nature, because secondary currents always show up, even in straight prismatic channels. This is one reason to perform 3D simulations, which are able to reconstruct the 3D velocity field and to test the robustness of the formula with respect to the (conceptual) model error. In the validation test n. 3 we compare the vertically averaged velocity components along the river bed direction computed by the 3D model with the values obtained by our formulas. The 3D configuration more close to the uniform flow approximation is the one envisaged by setting the average water depth in the most upstream water section equal to the downstream one, which is given as boundary condition.

Question 10) page 2628, point 2 line 11: I didn't see any proof that the estimation of β (to □9) is still valid for real rivers.

Reply: Our strategy, in this and other challenges for the prediction and the observation of natural variables, is to perceive a rigorous scientific approach, even in the consciousness that heterogeneity and uncertainty in nature do not allow a precise estimation of the predicted/monitored variables. We agree with the reviewer that the accuracy attained

in the results of lab experiments, carried out in small channels at least one order of magnitude smaller than the real rivers, with geometry and roughness very well known, cannot be assumed to be the same holding for real rivers. On the other hand, I would personally never apply for discharge estimation a formula that doesn't work at least in the lab. The other two tests are aimed to partially overcome the previously mentioned limit by a) validating the formula in the context of the indirect discharge estimation methodology, b) validating the formula by comparison of the estimated vertically averaged velocities with the results computed by a fully 3D model.

Question 11) *table 5: it is strange to want a Manning coefficient which can vary with the water level but must remain constant along a river reach 13 km long. How to be sure that the roughness is constant throughout 13 km?*

Reply: See the second part of the reply to Question 1.

Question 12) *table 6: this table does not clearly prove that IDCM, INCM and LHRM does better than DCM, the differences are too small to be convincing.*

Reply: We agree with the reviewer that the results of Validation test 2 are good for all the compared formulas, even if LHRM results match the measured values a little bit better. A possible explanation is that the indirect discharge estimation is based on the conservation of the wave volume and this depends on both the estimated wave celerity and on the storage occurring inside the reach along the observation time. The Manning coefficient and the water depth – discharge relationship affect only the celerity estimation. The Alzette river has a relatively small bed slope in the investigated reach (~0.08%) and this provides a relatively small sensitivity of the results with respect to the selected formula.
On the other hand we can see in tables 3 and 8 that LHRM provides results that are better than results of traditional methods DCM and IDCM in all the validation tests, not only in test 2, and that the error in tests 1 and 3 is much smaller than the error obtained by the other formulas.

Question 13) *Figures 5 to 10 (graphs) would be more readable if they were in colors.*
Reply: We agree with the reviewer (and hope it won't cost too much…).

Reply to review of J.B. Faure (reviewer #1) after Editor initial decision letter

In his initial decision letter the editor says:

…The topic is original and is important for both hydraulic and hydrologic applications. Both reviewers raised important issues concerning the hypotheses, the dataset, the methodology, the results, the discussion and the domain of application of this new approach in Earth Sciences. I agree with the suggestion of Reviewer #1 for additional applications and discussion for example on "a use-case doing a link with another domain in Earth sciences which would make this paper more interesting for HESS readers"…...

In their responses, the authors give responses to some of the critics raised by the reviewers, but some important issues raised by reviewers still need complementary responses, such as showing the domain of applications of the method for hydrological applications, as for example to "evaluate local vertically averaged velocities in sub-sections and then compute bottom shear stresses" (see Reviewer #1).

We hope to have fulfilled the editor requirements by 1) expanding the focus of the paper not only on the discharge computation, but more generally on the computation of the vertically averaged velocities along a river cross section and 2) proving with specific references that this issue is fundamental for both flow routing models and solid transport computation in rivers.
To this end, we changed the title in: "*Computation of vertically averaged velocities in irregular sections of straight channels*" and we added, in the introduction, a short discussion about the use of the vertically averaged velocities in the flow routing model (see attached paper). Moreover, we

added in the conclusion a short discussion about its use in the solid transport computation. Unfortunately, all transport formulas available in literature have been developed and tested with reference to the solid flux per unit width and all the experiments have been carried out in flumes with large rectangular sections, where the vertically averaged velocities are obviously constant. In the cited section, we observe that the solid flux per unit with is assumed, according to many popular formulas, to be proportional to the volumetric flux exceeding a minimum value. This implies that the error in the total solid flux estimation is at least proportional to the same error, extensively discussed in the paper, resulting in the total volumetric flux (i.e. discharge) estimation due to the vertically averaged velocity distribution error.

Computation of vertically averaged velocities in irregular sections of straight channels

Reply to review of P. Rameshwaran (reviewer #2)

Previous reviews and replies

Reply n.1 to review of P. Rameshwaran (reviewer #2)

The authors would like first to thank the reviewer for his valuable job.

Question 1): *The title - Uniform flow formulas for irregular sections - suggests that the new methods are applicable to all planform rivers (i.e. straight, meander and skewed simple or compound rivers) but the sections up to 4 are only deals with straight simple (K4 case?) or compound channels (other cases). Are these methods applicable to all planform rivers?*
Reply: The reviewer is right. In the paper we didn't investigated the effect of meandering. We referred only to straight channels, even if formulas for straight channels are usually extended also to meandering channels. We changed the title in "Uniform flow formulas for irregular sections in straight channels".

Question 2): *The SKM or similar methods can be numerically solved (see our paper with Ramesh waran & Shiono 2007) i.e. for irregular sections. You only need to discretized into linear elements for analytical solution only (lines 101 to 102).*
Reply: In the introduction we meant to say that analytical or approximated solutions require to neglect secondary flows. Of course, it is possible to carry on numerical integration along the lateral (y) direction of the vertically integrated Reynolds equation, like it is done with the SKM or similar methods. This doesn't avoid the need of using empirical parameters, required to compute the eddy viscosity. In the revised paper we corrected the text to and we added the missing reference.

Question 3): *In SKM papers, the friction factor is defined as f=8gRS/U^2 but some other papers including Huthoff et al. 2008, it is defined as f=gRS/U^2. The authors need to state their friction factor equation.*
Reply: Our friction coefficient is the same one used by Huthoff in his traditional approach ($f=gn^2/R^{1/3}$). In the paper the value of f shown in equation (8) was divided by the gravity acceleration, which was taken into account in the first term on the right side of equation (6). To avoid any ambiguity, we changed in the revised paper Eqs. (6) and (8) according to the previous definition of f.

Question 4): *Looking at 13 km Alzette study reach in Figure 4, It got variety of planform (straight, bend/curve, meander etc). In such cases, the energy losses not only form bed roughness elements but also from secondary flows due to planform and expansions and contractions in meandering. Are these methods applicable to the Alzette study reach? The authors need to clarify this.*
Reply: The Manning coefficient has, in the context of the indirect method for discharge estimation, the meaning of a calibration parameter, that we use to match the water levels measured in the downstream section with the level computed by the 1D hydraulic model.
It is well known from the parameter estimation theory (*Aster et al., 2012*) that in any numerical model the uncertainty of the estimated parameters, obtained by matching the computed and the measured model output, grows very quickly with the parameter number. This implies the need of minimizing the number of parameters, also by neglecting the effect of irregularities and heterogeneities. Of course, it would be very easy to fit very well the measured and the computed water level hydrographs (that are the output of the hydraulic model) also by differentiating the Manning coefficient along the reach or along the section, but the corresponding parameter error would become very large even with a small error in the topography or in the measured water levels. These errors strongly affect the discharge computed by the hydraulic model. Moreover, if the computed Manning coefficients or the parameters of other formulas were used for prediction purpose (which is a major benefit of the indirect measurement approach) the predicted discharges would be affected by an even stronger error. All this implies, of course, that test n.2 can be thought as the validation of the proposed formulas for their use in the specific method for the discharge estimation.
On the other hand, as explained in the paper, it is very difficult to carry on field tests for the validation of these formulas, because roughness coefficients are unknown and the results of all formulas can be scaled according to the

selected Manning coefficient or to other parameters. The indirect method provides a unique possibility of carrying on a simultaneous estimation of both the Manning coefficient and the discharge hydrograph.
In the revised paper we expanded the introduction to the indirect discharge measurement method, by adding:
" It is well-known in the parameter estimation theory (Aster et al., 2012) that the uncertainty of the estimated parameters (in our case the roughness coefficient) grows quickly with the number of parameters, even if the matching between the measured and the estimated model variables (in our case the water stages in the downstream section) improves. The use of only one single parameter over all the computational domain is motivated by the need of getting a robust estimation of the Manning's coefficient and of the corresponding discharge hydrograph."

Question 5): *Line 400, the length of the reach is about four times the top width of the section. Line 450, in the inlet section a constant velocity, normal to the section, is applied, and the pressure is left unknown. Is the length (i.e. using constant velocity inlet) enough for flow to develop within 3D model? The authors need to provide evidence.*
Reply: To address the reviewer concern, we carried out new computations to check the sensitivity of the estimated discharge with respect to the length of the prismatic reach. An extension of about 10% has been applied, increasing the size of the computational domain from about 20×10^6 to about 21×10^6 elements. The computed dimensionless sensitivity has been equal to:

$$S = \frac{L}{Q}\frac{\Delta Q}{\Delta L} = 0.002,$$

which we believe indicates a robust estimation, also because a small change in the results can be motivated also by the grid change. We added in the revised paper:
"Stability of the results has been checked against the variation of the length of the simulated channel. The dimensionless sensitivity of the discharge with respect to the channel length is equal to 0.2%".

Question 6): *Lines 460 to 462: CFX allows the use, inside the boundary layer, of a velocity logarithmic law, according to an equivalent granular size. What is the logarithmic d_{50} relationship used in CFX?*
Reply: The logarithmic wall law implemented in ANSYS CFX solver is the modified version of the Launder and Spalding (1974) log-law equation (Shen and Diplas, 2010; Ansys CFX-solver theory guide, Rel.14.0, 2006):

$$\frac{u}{u^*} = \frac{1}{k}\ln\left(\frac{c_\mu^{\frac{1}{4}} y k^{\frac{1}{2}}}{\nu}\right) - \frac{1}{k} ln\left(1 + \frac{0.15 d_{50} c_\mu^{\frac{1}{4}} k^{\frac{1}{2}}}{\nu}\right) + C$$

where:
c_μ = 0.09 is an empirical coefficient;
k= local turbulent kinetic energy;
ν= kinematic viscosity of the fluid;
d_{50}=average granular size;
C=log-layer constant dependent on wall roughness.

where the applied value d_{50} = 0.73 m has been selected according to its relationship with the *n* Manning coefficient, given by Eq. (27) (Yen, 1994).

Question 7): *What is the d_{50} value used? Is the logarithmic relationship and first (i.e. boundary mesh size) valid (see papers Nicholas, 2005; Lane et al., 2004; Carney et al., 2006, Rameshwaran et al. 2011)?*
Reply: Given that the logarithmic law is no longer valid for a distance from the boundary wall (*y*):
$y \leq 0.1\ d_{50}$
as reported inside "lecture notes on turbulence " (B. Mutlu Sumer, 2013), the authors decided to locate the first point of the mesh above the river bed at a distance *y* equal to 0.1 d_{50}=0.07m.

Reply n.2 to review of P. Rameshwaran (reviewer #2)

Reviewer comments:
1. Is this non-vegetated river?
Reply: No, there is vegetation both inside the river main channel and in the floodplains. As we said in the first review, a much larger number of parameters would have been required in order to provide a detailed reconstruction of the flow variables, but the goal of the proposed application is simply to prove that even the use of a single parameter (Manning coefficient) allows the computation, by means of the proposed formulas and of the indirect measurement strategy, of the actual river discharge.
2. Question (5) is all about flow development along the very short model length. Are the flow parameters (velocity, TKE, bed shear stress...) reached fully development state within the modeled length? The authors need to provide evidence of longitudinal profile of flow parameters (Longitudinal velocity, TKE, bed shear stress...) along the reach. Otherwise, they need to use fully developed condition at inlet boundary (see Rameshwaran et al. 2013 section 5)

Reply: We agree with the reviewer that the use of zero gradient boundary conditions at the outlet plane would be more appropriate for our simulations. On the other hand, the CFX code does not allow to prescribe this condition at the outlet plane. In the computations we followed the reviewer strategy only in the first part, because we adjusted the velocity distribution in the inlet plane according to the result of a previous steady-state simulation. In the outlet plane we set the hydrostatic pressure distribution, and assigned zero non-orthogonal components to the velocity.
In the first revised version we have shown that the sensitivity of the discharge, computed in the middle section, is anyway very low, such doubling the length of the modeled channel would provide an increment of less than 0.2% of the computed discharge.
In the revised paper we added the following comment about the chosen boundary conditions:
"A more appropriate boundary condition at the outlet section, not available in the CFX code, would have been given by zero velocity and turbulence gradients (Rameshwaran et al. 2013)".
In order to test the achievement of the fully developed state within the first half of the modeled length the authors plotted the vertical profiles of the streamwise velocity components for ten verticals, equally spaced along the longitudinal axis of the main channel. See in Fig. 1 the plot of five of them and their location. The streamwise velocity evolves longitudinally and becomes almost completely self similar starting from the vertical line in the middle section (p5 velocity profile). This means that the boundary layer, and so the flow, is fully developed since the middle section. We expanded the computational domain further on only to show the secondary currents computed in the middle section.
In the revised paper we added the plot and the following comments:
"To compute the uniform flow discharge, for a given outlet section, CFX code is run iteratively, each time with a different average longitudinal velocity in the inlet section, until the same water depth as in the outlet section is attained in the inlet section for steady state conditions. Using the velocity distribution computed in the middle section along the steady state computation as upstream boundary condition, transient analysis is carried on until pressure and velocity oscillations become periodic."
"In order to test the achievement of the fully developed state within the first half of the modeled length the authors also plotted the vertical profiles of the streamwise velocity components for ten verticals, equally spaced along the longitudinal axis of the main channel. See in Fig. 15 the plot of five of them and their location. The streamwise velocity evolves longitudinally and becomes almost completely self similar starting from the vertical line in the middle section."

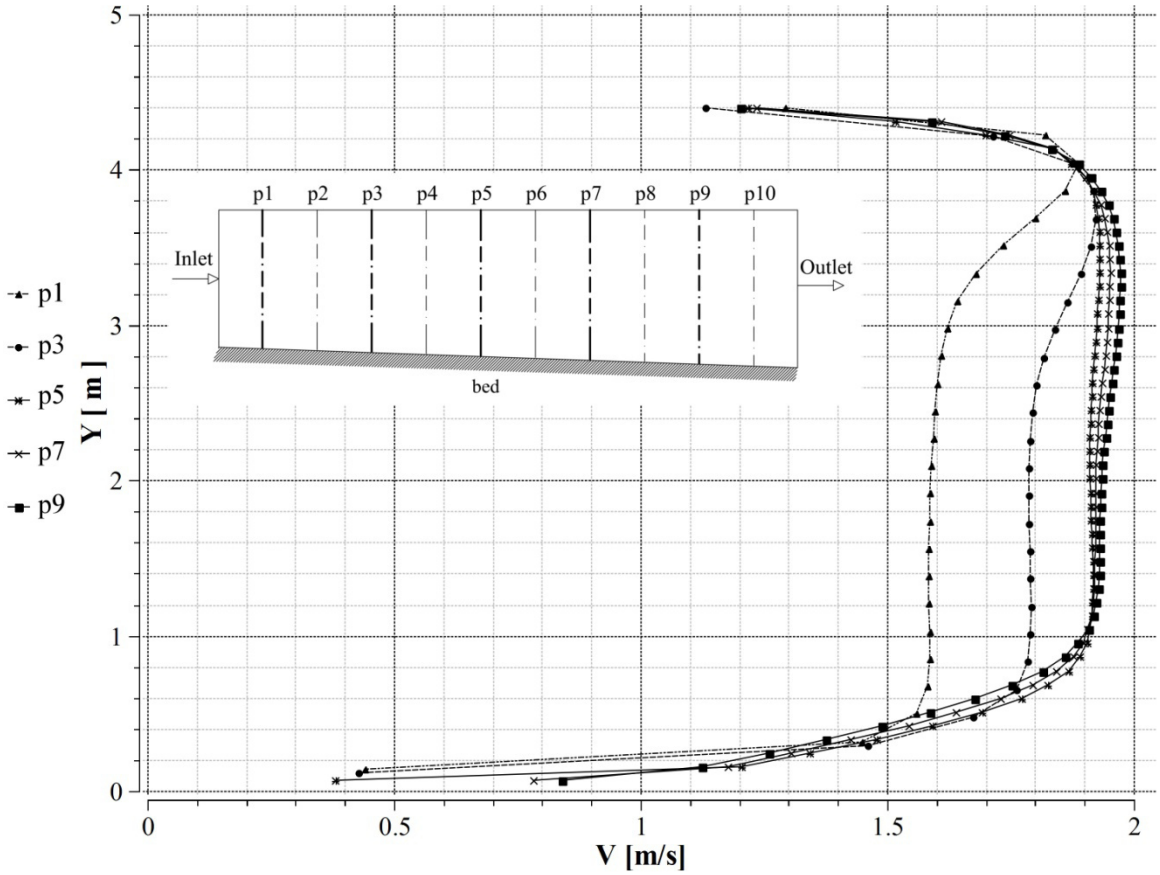

Fig. 1. Streamwise vertical profile along the longitudinal axis of the mean channel.

References

Rameshwaran, Ponnambalam; Naden, Pamela; Wilson, Catherine A.M.E.; Malki, Rami; Shukla, Deepak R.; Shiono, Koji. 2013 Inter-comparison and validation of computational fluid dynamics codes in two-stage meandering channel flows. Applied Mathematical Modelling, 37 (20-21). 8652-8672. 10.1016/j.apm.2013.07.016

Reviewer comments:
3. Question (6 & 7) and answer (6 & 7): The equation can be simplified ignoring some small terms as (correct me if I am wrong): u/u*=(1/k)ln(y/0.15d50)+C where d50=0.73 m and y=0.07 - What is your y+? Using above k=0.41: u/u*= -1.091291+C The above equation is meaningless unless C is positive and greater than 1.091291. What is C? (Refer to Introduction section in Rameshwaran et al. 2011 and other papers in my earlier comments). The first term is negative in the equation because the y is too small and d50 too big. It is therefore not numerically valid to use wall function approach to model flow over gravel beds with d50 = 0.73 m (see papers in my earlier comments).

Reply: In the previous review the authors reported the logarithmic wall law used in CFX solver as it has been shown in the study of Shen and Diplas (2010):

$$\frac{u}{u^*} = \frac{1}{\boldsymbol{k}}\ln\left(\frac{c_\mu^{\frac{1}{4}} y k^{\frac{1}{2}}}{\nu}\right) - \frac{1}{\boldsymbol{k}} ln\left(1 + \frac{0.15 d_{50} c_\mu^{\frac{1}{4}} k^{\frac{1}{2}}}{\nu}\right) + C \quad (1).$$

In the ANSYS CFX theory guide the log-law is expressed as follow:

$$\frac{u}{u^*} = \frac{1}{\boldsymbol{k}}\ln(y^+) + B - \Delta B \quad (2)$$

where $\boldsymbol{k}$ = 0.41 is the Von Karman constant;$\Delta B = \frac{1}{\boldsymbol{k}} ln(1 + 0.3 {h_s}^+)$ is the function of the dimensionless roughness height ${h_s}^+$ defined as :${h_s}^+ = \frac{h_s u^*}{\nu}$, B is a log constant equal to 5.2, $u^* = c_\mu^{\frac{1}{4}} k^{\frac{1}{2}}$and y^+ is the dimensionless distance from the boundary wall, defined as $\frac{y\, u^*}{\nu}$.

With appropriate substitutions we get from Eq. (2):

$$\frac{u}{u^*} = \frac{1}{\boldsymbol{k}} ln\left(\frac{c_\mu^{\frac{1}{4}} k^{\frac{1}{2}} y}{\nu}\right) + B - \frac{1}{\boldsymbol{k}} ln\left(1 + 0.3\frac{h_s c_\mu^{\frac{1}{4}} k^{\frac{1}{2}}}{\nu}\right) \quad (3).$$

Because$h_s = 0.5 * d_{50}$ Eq.(3) becomes:

$$\frac{u}{u^*} = \frac{1}{\boldsymbol{k}}\ln\left(\frac{c_\mu^{\frac{1}{4}} k^{\frac{1}{2}} y}{\nu}\right) + B - \frac{1}{\boldsymbol{k}} ln\left(1 + \frac{0.15 d_{50} c_\mu^{\frac{1}{4}} k^{\frac{1}{2}}}{\nu}\right) \quad (4).$$

Because Eq.(4) is equal to the Eq. (1), as observed in the previous reply, coefficient *C* is equal to *B* (equal to 5.2) and the ratio u/u* is positive.

Reply n.3 to review of P. Rameshwaran (reviewer #2)

Reviewer comments:
Three-dimensional modeling needs to be corrected or removed before publication.
1. Something fundamentally wrong with your 3D simulation with CFX. It can be seen from your "Fig. 1. Streamwise vertical profile along the longitudinal axis of the mean channel" that your vertical velocity profiles are not logarithmic and they are decreasing (turning back) near the free surface. The modelled part of your river is almost straight and without any vegetation where you expect almost logarithmic velocity profiles (see simulated profiles in Anderson et al., 2014, Rameshwaran et al, 2011, Shen and Diplas 2010).
2. Application of Ansys (2010) method needs to be sorted. In Anderson et al. (2014), Ansys (2010) method was applied on irregular river bed geometry mesh. Your bed seems to be flat in the simulation (like smooth ks case of Anderson et al., 2014). Is the Ansys (2010) method applicable for your case?

Reply 1. : We apologize first for the bad representation we gave of the computed velocity vertical profile. CFX solves the velocity field in a fixed domain containing also a volume above the free surface, on the assumption of common velocity for both air and liquid phase in each shared geometrical point (Nichols and Hirt 1975, Hirt and Nichols 1981). The velocity profile of the liquid
domain has to be cut, of course, at the level with zero relative pressure, as we did in the revised version of the paper (see Fig.1). Moreover, we improved the simulation by increasing the number of
the prismatic layers close the bottom. In Fig 1, we can see the profiles plotted in the semi-logarithmic space, showing a linear trend in the transition layer between the bottom and the fully developed turbulent velocity. No change has been observed with the new simulation in the computed distribution of the vertically averaged velocities along the lateral direction.

Reply 2. : The Ansys CFX code has shown a large reliability in the solution of turbulence problems,

also in the shallow water case. Moreover, the main focus of the paper is not about the optimal reconstruction of the 3D velocity field in the specific test case, but about the similarity of the results obtained in the estimation of the vertically averaged velocities by the new formulas with the same results obtained by a 3D code.

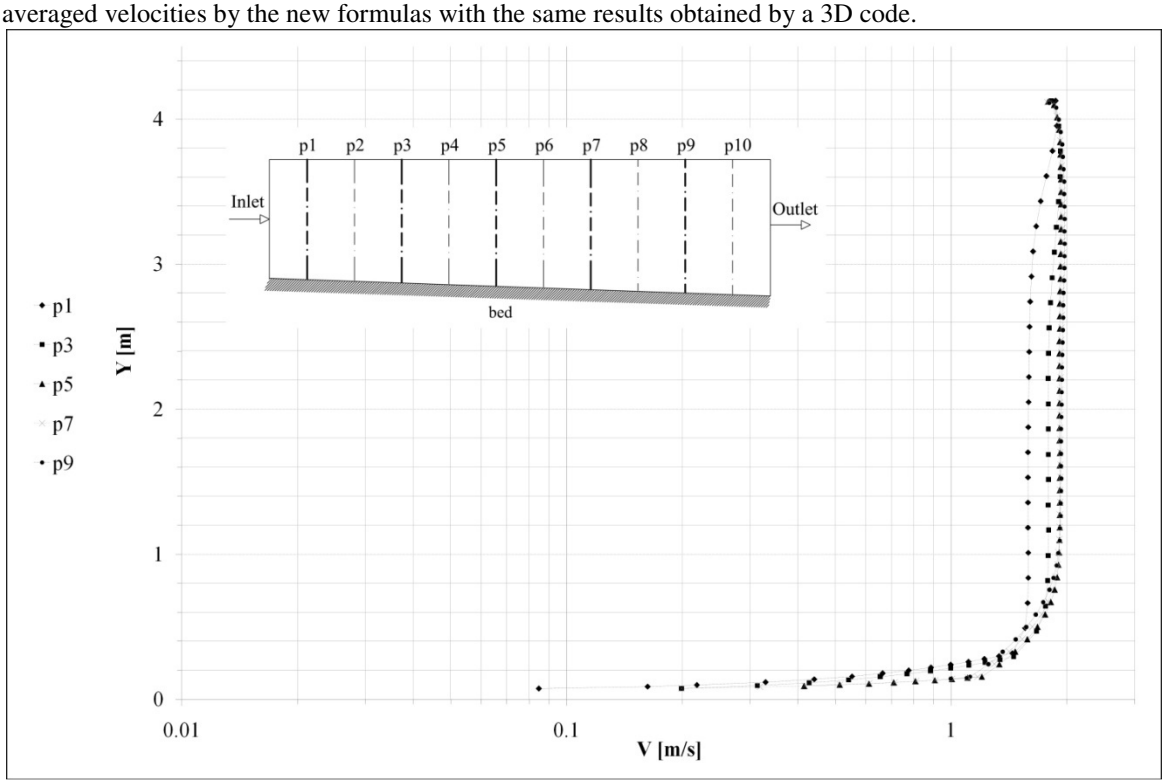

Fig. 1. Streamwise vertical profile along the longitudinal axis of the mean channel.

Reply to review of P. Rameshwaran (reviewer #2) after Editor initial decision letter

In his initial decision letter the editor says:

Both reviewers raised important issues concerning the hypotheses, the dataset, the methodology, the results, the discussion and the domain of application of this new approach in Earth Sciences. I agree with the suggestion of Reviewer #1…and the suggestion of Reviewer #2 to clearly indicate the objectives of the study and the domain of applications by modifying the title, the objectives and the related sections in the paper.

We hope to have fulfilled to the editor requirements by: 1) expanding the focus of the paper not only on the discharge computation, but more generally on the computation of the vertically averaged velocities along a river cross section and 2) proving with specific references that this issue is fundamental for both flow routing models and solid transport computation in rivers.
To this end, we changed the title in: "*Computation of vertically averaged velocities in irregular sections of straight channels*" and we added, in the introduction, a short discussion about the use of the vertically averaged velocities in the flow routing model (see attached paper). Moreover, we added in the conclusion a short discussion about its use in the solid transport computation. Unfortunately, all transport formulas available in literature have been developed and tested with reference to the solid flux per unit width and all the experiments have been carried out in flumes with large rectangular sections, where the vertically averaged velocities are obviously constant. In the cited section, we observe that the solid flux per unit with is assumed, according to many popular formulas, to be proportional to the volumetric flux exceeding a minimum value. This implies that the error in the total solid flux estimation is at least proportional to the same error, extensively

discussed in the paper, resulting in the total volumetric flux (i.e. discharge) estimation due to the vertically averaged velocity distribution error.

Computation of vertically averaged velocities in irregular sections of straight channels

ELEONORA SPADA, PhDstudent, *Dipartimento di Ingegneria Civile, Ambientale,Aerospaziale, dei Materiali (DICAM),Università degli studi di Palermo, Viale delle scienze, 90128, Palermo, Italy.*

Email: eleonora.spada@unipa.it (author for correspondence)

TULLIO TUCCIARELLI , Professor, *Dipartimento di Ingegneria Civile, Ambientale,Aerospaziale, dei Materiali (DICAM),Università degli studi di Palermo, Viale delle scienze, 90128, Palermo, Italy.*

Email: tullio.tucciarelli@unipa.it

MARCO SINAGRA , PhD, *Dipartimento di Ingegneria Civile, Ambientale,Aerospaziale, dei Materiali (DICAM),Università degli studi di Palermo, Viale delle scienze, 90128, Palermo, Italy.*

VINCENZO SAMMARTANO, PhD, *Dipartimento di Ingegneria Civile, dell'Energia, dell'Ambiente e dei Materiali (DICEAM), Università Mediterranea di Reggio Calabria, Via Graziella, 89122, Reggio Calabria, Italy.*

GIOVANNI CORATO, Researcher, Centre de Recherche Public 'Gabriel Lippmann',41 rue du Brill, L-4422 Belvaux, Luxembourg.

Computation of vertically averaged velocities in irregular sections of straight channels

ABSTRACT

Two new methods for vertically averaged velocity computation are presented, validated and compared with other available formulas. The first method derives from the well-known Huthoff algorithm, which is first shown to be dependent on the way the river cross-section is discretized into several sub-sections. The second method assumes the vertically averaged longitudinal velocity to be a function only of the friction factor and of the so-called "local hydraulic radius", computed as the ratio between the integral of the elementary areas around a given vertical and the integral of the elementary solid boundaries around the same vertical. Both integrals are weighted with a linear shape function, equal to zero at a distance from the integration variable which is proportional to the water depth according to an empirical coefficient β. Both formulas are validated against 1) laboratory experimental data, 2) discharge hydrographs measured in a real site, where the friction factor is estimated from an unsteady-state analysis of water levels recorded in two different river cross sections, 3) the 3D solution obtained using the commercial ANSYS CFX code, computing the steady state uniform flow in a cross section of the Alzette river.

Keywords: diffusive model,discharge estimation, irregular section, rating curve, uniform flow.

1 Introduction

Computation of vertically averaged velocities is the first step of two major calculations in 1D shallow water modelling: 1) estimation of the discharge given the energy slope and the water stage and 2) estimation of the bottom shear stress for computing the bed load in a given river section.

Many popular software tools, like MIKE11 (MIKE11, 2009), compute the discharge Q, in each river section, as the sum of discharges computed in different sub-sections, assuming a single water stage for all of them. Similarly, HEC-RAS (HEC-RAS,2010) calculates the conveyance of the cross-section by the following form of Manning's equation:

$$Q = KS_f^{1/2} \quad (1),$$

where S_f is the energy slope and K is the conveyance, computed assuming the same hypothesis and solving each sub-section according to the traditional Manning equation.

The uniform flow formula almost universally applied in each sub-section is still the Chezy equation (Herschel, C., 1897). The advantage of using the Chezy equation is that the associated Manning's coefficient has been calibrated worldwide for several types of bed surface and a single value is ready to use for each application. However, it is well known that the Chezy equation was derived from laboratory measurements taken in channels with a regular, convex cross-sectional shape. When the section results from the union of different parts, each with a strongly different average water depth, one of two options is usually selected. The first option, called Single Channel Method (SCM) is simply to ignore the problem. This leads to strong underestimation of the discharge, because the Chezy formula assumes a homogeneous vertically averaged velocity and this homogeneous value provides strong energy dissipation in the parts of the section with lower water depths. The second option, called Divided Channel Method (*DCM*) is to compute the total discharge as the sum of the discharges flowing in each convex part of the section (called subsection) , assuming a single water level for all parts (Chow 1959; Shiono et al. 1999; Myers and Brennan, 1990). In this approach, the wet perimeter of each subsection is restricted to the component of the original one pertaining to the subsection, but the new components shared by each couple of subsections are neglected. This is equivalent to neglecting the shear stresses coming from the vortices with vertical axes (if subsections are divided by

vertical lines) and considering additional resistance for higher velocities, which results in overestimation of discharge capacity (Lyness et al. 2001).

Knight and Hamed (1984) compared the accuracy of several subdivision methods for compound straight channels by including or excluding the vertical division line in the computation of the wetted perimeters of the main channel and the floodplains. However, their results show that conventional calculation methods result in larger errors. Wormleaton et al. (1982) and Wormleaton and Hadjipanos(1985) also discussed, in the case of compound sections, the horizontal division through the junction point between the main channel and the floodplains. Their studies show that these subdivision methods cannot well assess the discharge in compound channels.

The interaction phenomenon in compound channels has also extensively studied by many other researchers (e.g., Sellin 1964; Knight and Demetriou 1983; Stephenson and Kolovopoulos 1990; Rhodes and Knight 1994; Bousmar and Zech 1999; van Prooijen et al. 2005; Moreta and Martin-Vide 2010). These studies demonstrate that there is a large velocity difference between the main channel and the floodplain, especially at low relative depth, leading to a significant lateral momentum transfer. The studies by Knight and Hamed(1984), Wormleaton et al. (1982) indicate that vertical transfer of momentum between the upper and the lower main channels exists, causing significant horizontal shear able to dissipate a large part of the flow energy.

Furthermore, many authors have tried to quantify flow interaction among the subsections, at least in the case of compound, but regular channels. To this end turbulent stress was modelled through the Reynolds equations and coupled with the continuity equation (Shiono and Knight, 1991). This coupling leads to equations that can be analytically solved only under the assumption of negligible secondary flows. Approximated solutions can also be obtained, although they are based on some empirical parameters. Shiono and Knight developed the Shiono-Knight Method (*SKM*) for prediction of lateral distribution of depth-averaged velocities and boundary shear stress in prismatic compound channels (Shiono and Knight, 1991; Knight and Shiono, 1996). The method can deal with all channel shapes that can be discretized into linear elements (Knight and Abril, 1996; Abril and Knight, 2004).

Other studies based on the Shiono and Knight method can be found in Liao and Knight (2007), Rameshwaran and Sjiono (2007), Tang and Knight (2008) and Omran and Knight (2010). Apart from *SKM*, some other methods for analysing the conveyance capacity of compound channels have been proposed. For example,

Ackers (1993) formulated the so called empirical coherence method. Lambert and Sellin(1996) suggested a mixing length approach at the interface, whereas more recently Cao et al. (2006) reformulated flow resistance through lateral integration using a simple and rational function of depth-averaged velocity. Bousmar and Zech (1999) considered the main channel/floodplain momentum transfer proportional to the product of the velocity gradient at the interface times the mass discharge exchanged through this interface due to turbulence. This method, called *EDM*, also requires a geometrical exchange correction factor and turbulent exchange model coefficient for evaluating discharge.

A simplified version of the *EDM*, called Interactive Divided Channel Method (*IDCM*), was proposed by Huthoff et al. (2008). In *IDCM* lateral momentum is considered negligible and turbulent stress at the interface is assumed to be proportional to the span wise kinetic energy gradient through a dimensionless empirical parameter α. *IDCM* has the strong advantage of using only two parameters, α and the friction factor, *f*. Nevertheless, as shown in the next section, α depends on the way the original section is divided.

An alternative approach could be to simulate the flow structure in its complexity by using a three-dimensional code for computational fluid dynamics (CFD). In these codes flow is represented both in terms of transport motion (mean flow) and turbulence by solving the Reynolds Averaged Navier Stokes (RANS) equations (Wilcox, 2006) coupled with turbulence models. These models allow closure of the mathematical problem by adding a certain number of additional partial differential transport equations equal to the order of the model. In the field of the simulation of industrial and environmental laws second order models (e.g. k-ε and k-ω models) are widely used. Nonetheless, CFD codes need a mesh fine enough to solve the boundary layer (Wilcox, 2006), resulting in a computational cost that can be prohibitive even for river of few km.

In this study two new methods, aimed to represent subsection interactions in a compound channel, are presented. The first method, named "INtegrated Channel Method" (*INCM*), derives from the previous Huthoff formula, which is shown to give results depending on the way the river cross section is discretized in sub-sections. The same dynamic balance adopted by Huthoff is written in differential form, but its

149 diffusive term is weighted according to a ξ coefficient proportional to the local water
150 depth.
151 The second one, named “local hydraulic radius method” (*LHRM*), derives from the
152 observation that, in the Manning formula, the mean velocity per unit energy gradient
153 is proportional to a power of the hydraulic radius. It should then be possible to get the
154 vertically averaged velocity along each vertical by using the same Manning formula,
155 where the original hydraulic radius is changed with a "local" one. This "local"
156 hydraulic radius should take into account the effect of the surrounding section
157 geometry, up to a maximum distance which is likely to be proportional to the local
158 water depth, according to an empirical β coefficient. The method gives up the idea of
159 solving the Reynolds equations, due to the uncertainty of its parameters, but relies on
160 the solid grounds of the historical experience of the Manning equation.
161 The present paper is organized as follows: Two of the most popular approaches
162 adopted for computation of the vertically averaged velocities are explained in details,
163 along with the proposed *INCM* and *LHRM* methods. The ξ and β parameters of
164 respectively the *INCM* and *LHRM* methods are then calibrated from available
165 discharge lab experimental data and a sensitivity analysis is carried out. The *INCM*
166 and *LHRM* methods are finally validated according to three different criteria. The first
167 criterion is comparison with other series of the previous laboratory data, not used for
168 calibration. The second criterion is comparison with discharge data measured in one
169 section of the Alzette river Basin (Luxembourg). Because the friction factor is not
170 known a priori, *INCM* and *LHRM* formulas are applied in the context of the indirect
171 discharge estimation method, which simultaneously estimates the friction factor and
172 the discharge hydrograph from the unsteady state water level analysis of two water
173 level hydrographs measured in two different river sections. The third validation
174 criterion is comparison with the vertical velocity profiles obtained by the ANSYS
175 CFX solver, in a cross section of the Alzette river. In the conclusions, it is finally
176 shown that application of bed load formulas, carried out by integration of elementary
177 solid fluxes computed as function of the vertically averaged velocities, can lead to
178 results that are strongly different from those obtained by using the simple mean
179 velocity and water depth section values.

2 Divided Channel Method (*DCM*) and Interactive Divided Channel Method (*IDCM*)

In the *DCM* method the river section is divided into subsections with uniform velocities and roughness (Chow, 1959). Division is made by vertical lines and no interaction between adjacent subsections is considered. Discharge is obtained by summing the contributions of each subsection, obtained by applying the Manning formula:

$$q = \sum_i q_i = \sum_i \frac{R_i^{2/3} A_i}{n_i} \sqrt{S_f} \quad (2),$$

where q is the total discharge, A_i , R_i and n_i are the area, the hydraulic radius and the Manning's roughness coefficient of each sub section i of a compound channel and S_f is the energy slope, assumed constant across the river section. *DCM* is extensively applied in most of the commercial codes, two of them cited in the introduction.

In order to model the interaction between adjacent subsections of a compound section, the Reynolds and the continuity equations can be coupled (Shiono and Knight, 1991), to get:

$$\rho \frac{\partial}{\partial y}\left(H \overline{U}_v \overline{V}_d\right) = \rho g H S_0 + \frac{\partial}{\partial y}\left(H \bar{\tau}_{xy}\right) - \tau_b \left(1 + \frac{1}{s^2}\right)^{1/2} \quad (3),$$

where ρ is the water density, g is the gravity acceleration, y is the abscissa according to the lateral direction, U and V are respectively the velocity components along the flow x direction and the lateral y direction, H is the water depth, the sub-index d marks the vertically averaged quantities and the bar the time average along the turbulence period, S_0 is the bed slope, s is the section lateral slope, and τ_β is the bed shear stress. The $\bar{\tau}_{xy}$ turbulent stress is given by the eddy viscosity equation, that is:

$$\bar{\tau}_{xy} = \rho \bar{\varepsilon}_{xy} \frac{\partial U_d}{\partial y} \quad (4a),$$

$$\bar{\varepsilon}_{xy} = \lambda U_* H \quad (4b),$$

where the friction velocity U_* is set equal to:

$$U_* = \left(\frac{f}{8g}\right)^{1/2} U_d \quad (5),$$

206 and f is the friction factor, depending on the bed material. The analytical solution of
207 Eqs. (3)-(5) can be found only if the left hand side of Eq. (3) is zero, which is
208 equivalent to neglecting secondary flows. Other solutions can only be found by
209 assuming a known Γ value for the lateral derivative. Moreover, λ is another
210 experimental factor depending on the section geometry. The result is that solution of
211 Eq. (3) strongly depends on the choice of two coefficients, λ and Γ, which are
212 additional unknowns with respect to the friction factor *f*.
213 In order to reduce to one the number of empirical parameters (in addition to *f*) Huthoff
214 et al. (2008) proposed the so-called Interactive Divided Channel Method (*IDCM*).
215 Integration of Eq. (3) over each i^{th} subsection, neglecting the averaged flow lateral
216 momentum, leads to:

217 $$\rho g A_i S_0 = \rho f_i P_i U_i^2 + \tau_{i+1} H_{i+1} + \tau_i H_i \qquad (6),$$

218 where the left-hand side of Eq.(6) is the gravitational force per unit length,
219 proportional to the density of water ρ, to the gravity acceleration g, to the cross-
220 sectional area A_i, and to the stream wise channel slope S_0. The terms at the right-hand
221 side are the friction forces, proportional to the friction factor f and to the wet solid
222 boundary P_i, as well as the turbulent lateral momentum on the left and right sides,
223 proportional to the turbulent stress τ and to the water depth H.
224 Turbulent stresses are modelled quite simply as:

225 $$\tau_{i+1} = \frac{1}{2}\rho\alpha\left(U_{i+1}^2 - U_i^2\right) \qquad (7),$$

226 where α is a dimensionless interface coefficient, $U^2{}_i$ is the square of the vertically
227 averaged velocity and τ_i is the turbulent stress along the plane between subsection *i-1*
228 and *i*. If subsection *i* is the first (or the last) one, velocity U_{i-1} (or U_{i+1}) is set equal to
229 zero.
230 Following a wall-resistance approach (Chow, 1959), the friction factor f_i is computed
231 as:

232 $$f_i = \frac{g\, n_i^2}{R_i^{1/3}} \qquad (8),$$

233 where n_i is the Manning's roughness coefficient and $R_i(=A_i/P_i)$ is the hydraulic radius
234 of subsection *i*.

Equations (6) forms a system with an order equal to the number m of subsections, which is linear in the U_i^2 unknowns. The results are affected by the choice of the α coefficient, which is recommended by Huthoff et al. (2008), on the basis of lab experiments, equal to 0.02. Computation of the velocities U_i makes it easy to estimate discharge q.

IDCM has the main advantage of using only two parameters, the f and α coefficients. On the other hand, it can be easily shown that α, although it is dimensionless, depends on the way the original section is divided. The reason is that the continuous form of Eq. (6) is given by:

$$\rho g\left(HS_0 - \frac{f\,U^2}{g\,cos\theta}\right) = \frac{\partial}{\partial y}(\tau H) \qquad (9),$$

where θ is the bed slope in the lateral direction. Following the same approach as the *IDCM*, if we assume the turbulent stress τ to be proportional to both the velocity gradient in the lateral direction and to the velocity itself, we can write the right-hand side of Eq. (9) in the form:

$$\frac{\partial}{\partial y}(\tau H) = \frac{\partial}{\partial y}\left(\frac{\alpha_H}{2}\rho U\frac{\partial U}{\partial y}H\right) \qquad (10),$$

and Eq. (9) becomes:

$$\rho\left(gHS_0 - \frac{f\,U^2}{g\,cos\theta}\right) = \frac{\partial}{\partial y}\left(H\frac{\partial}{\partial y}\left(\alpha_H\rho U^2\right)\right) \qquad (11).$$

In Eq. (10) α_H is no longer dimensionless, but is a length. To get the same Huthoff formula from numerical discretization of Eq. (10), we should set:

$$\alpha_H = 0.02\,\Delta y \qquad (12),$$

where Δy is the subsection width, i.e. the integration step size. This implies that the solution of Eq. (11), according to the Huthoff formula, depends on the way the equation is discretized and the turbulence stress term on the r.h.s. vanishes along with the integration step size.

3 The new methods

3.1 Integrated Channel Method (INCM)

INCM derives from the *IDCM* idea of evaluating the turbulent stresses as proportional to the gradient of the squared averaged velocities, leading to Eqs. (7) and (11). Observe that dimensionless coefficient α, in the stress computation given by Eq. (7), can be written as the ratio between α_H and the distance between verticals *i* and *i+1*. For this reason, coefficient α_H can be thought of as a sort of mixing length, related to the scale of the vortices with horizontal axes. *INCM* assumes the optimal α_H to be proportional to the local water depth, because water depth is at least an upper limit for this scale, and the following relationship is applied:

$$\alpha_H = \xi H \quad (13),$$

where ξ is an empirical coefficient to be further estimated.

3.2 Local hydraulic radius method (LHRM)

LHRM derives from the observation that, in the Manning equation, the average velocity is set equal to:

$$V = \frac{R^{2/3}}{n}\sqrt{S_0} \quad (14),$$

and has a one-to-one relationship with the hydraulic radius. In this context the hydraulic radius has the meaning of a global parameter, measuring the interactions of the particles along all the section as the ratio between an area and a length. The inconvenience is that, according to Eq. (14), the vertically averaged velocities in points very far from each other remain linked anyway, because the infinitesimal area and the infinitesimal length around two verticals are summed to the numerator and to the denominator of the hydraulic radius independently from the distance between the two verticals. To avoid this, *LHRM* computes the discharge as an integral of the vertically averaged velocities, in the following form:

$$q = \int_0^L h(y)U(y)dy \quad (15),$$

where *U* is set equal to:

$$U = \frac{\Re_l^{2/3}}{n}\sqrt{S_0} \tag{16},$$

and $\Re_l$ is defined as local hydraulic radius, computed as:

$$\Re_l(y) = \frac{\int_a^b h(s)\,N(y,s)\,ds}{\int_a^b N(y,s)\sqrt{ds^2+dz^2}} \tag{17a},$$

$$a = \max(0,\ y-\beta h) \tag{17b},$$

$$b = \min(L,\ y+\beta h) \tag{17c},$$

where z is the topographic elevation (function of s), β is an empirical coefficient and L is the section top width. Moreover $N(y, s)$ is a shape function where:

$$N(y,s) = \begin{cases} -\dfrac{[y-\beta h(y)]-s}{\beta h(y)} & \text{if} \quad a<s<y \\ \dfrac{[y-\beta h(y)]-s}{\beta h(y)} & \text{if} \quad b>s>y \\ 0 & \text{otherwise} \end{cases} \tag{18}.$$

Equations (18) show how the influence of the section geometry, far from the abscissa y, continuously decreases up to a maximum distance, which is proportional to the water depth according to an empirical positive coefficient β. After numerical discretization, Eqs (15)-(17) can be solved to get the unknown q, as well as the vertically averaged velocities in each subsection. If β is close to zero and the size of each subsection is common for both formulas, LHRM is equivalent to DCM; if β is very large LHRM is equivalent to the traditional Manning formula. In the following, β is calibrated using experimental data available in the literature. A sensitivity analysis is also carried out, to show that the estimated discharge is only weakly dependent on the choice of the β coefficient, far from its possible extreme values.

3.3 Evaluation of the ξ and β parameters by means of lab experimental data

INCM and *LHRM* parameters were calibrated by using data selected from six series of experiments run at the large scale Flood Channel Facility (FCF) of HR Wallingford (UK), (Knight and Sellin, 1987; Shiono and Knight, 1991; Ackers, 1993), as well as

from four series of experiments run in the small-scale experimental apparatus of the Civil Engineering Department at the University of Birmingham (Knight and Demetriou, 1983). The FCF series were named F1, F2, F3, F6, F8 and F10; the Knight and Demetriou series were named K1, K2, K3 and K4. Series F1, F2, and F3 covered different floodplain widths, while series F2, F8, and F10 kept the floodplain widths constant, but covered different main channel side slopes. Series F2 and F6 provided a comparison between the symmetric case of two floodplains and the asymmetric case of a single floodplain. All the experiments of Knight and Demetriou (1983) were run with a vertical main channel wall, but with different B/b ratios. The series K1 has B/b = 1 and its section is simply rectangular. The B/b ratio, for Knight's experimental apparatus, was varied by adding an adjustable side wall to each of the floodplains either in pairs or singly to obtain a symmetrical or asymmetrical cross section. The geometric and hydraulic parameters are shown in Table 1; all notations of the parameters can be found in Fig. 1 and S_0 is the bed slope. The subscripts "mc" and "fp" of the side slope refer to the main channel and floodplain, respectively. Perspex was used for both main flume and floodplains in all tests. The related Manning roughness is 0.01 $m^{-1/3}s$.

The experiments were run with several channel configurations, differing mainly for floodplain geometry (widths and side slopes) and main channel side slopes (see Table 1). The K series were characterized by vertical main channel walls. More information concerning the experimental setup can be found in Table 1 (Knight and Demetriou, 1983; Knight and Sellin, 1987; Shiono and Knight, 1991).

Four series, named F1, F2, F3 and F6, were selected for calibration of the β coefficient, using the Nash Sutcliffe (NS) index of the measured and the computed flow rates as a measure of the model's performance (Nash and Sutcliffe, 1970).

The remaining three series, named F2, F8 and F10, plus four series from Knight and Demetriou, named K1, K2, K3 and K4, were used for validation (no.) 1, as reported in the next section. NS is given by:

$$NS = \left[1 - \frac{\sum_{j=1,2} \sum_{i=1,N_J} \sum_{K=1,M_{N_J}} (q_{i,j,k}^{obs} - q_{i,j,k}^{sim})^2}{\sum_{j=1,2} \sum_{i=1,N_J} \sum_{K=1,M_{N_J}} (q_{i,j,k}^{obs} - \overline{q_{i,j,k}^{obs}})^2} \right] \quad (19),$$

where N_j is the number of series, M_{Nj} is the number of tests for each series, $q^{sim}{}_{i,j,k}$ and $q^{obs}{}_{i,j,k}$ are respectively the computed and the observed discharge (j = 1 for the

FCF series and j = 2 for the Knight series; i is the series index and K is the water depth index). $\overline{q_{i,j,k}^{obs}}$ is the average value of the measured discharges.

Both ξ and β parameters were calibrated by maximizing the Nash Sutcliffe (NS) index, computed using all the data of the four series used for calibration. See the NS versus ξ and β curves in Figs. 2a and 2b.

Calibration provides optimal ξ and β coefficients respectively equal to 0.08 and 9. The authors will show in the next sensitivity analysis that even a one-digit approximation of the ξ and β coefficients provides a stable discharge estimation.

3.4 Sensitivity analysis

We carried out a discharge sensitivity analysis of both new methods using the computed ξ = 0.08 and β=9 optimal values and the data of the F2 and K4 series. Sensitivities were normalized in the following form:

$$I_s = \frac{1}{q_{INCM}} \frac{\Delta q}{\Delta \xi} \quad (20),$$

$$L_s = \frac{1}{q_{LHRM}} \frac{\Delta q}{\Delta \beta} \quad (21),$$

where Δq is the difference between the discharges computed using two different β and ξ values. The assumed perturbations"Δβ" and "Δξ" are respectively Δβ = 0.001 β, Δξ = 0.001 ξ.

The results of this analysis are shown in Table 2a for the F2 series, where H is the water depth and Q_{meas} the corresponding measured discharge.

They show very low sensitivity of both the *INCM* and *LHRM* results, such that a one digit approximation of both model parameters (ξ and β) should guarantee a computed discharge variability of less than 2%.

The results of the sensitivity analysis, carried out for series K4 and shown in Table 2b, are similar to the previous ones computed for F2 series.

4 Validation criterion

4.1 Validation n.1 - Comparison with laboratory experimental data

A first validation of the two methods was carried out by using the calibrated parameter values, the same Nash-Sutcliffe performance measure and all the available experimental series. The results were also compared with results of *DCM* and *IDCM* methods, the latter applied using the suggested $\alpha = 0.02$ value and five subsections, each one corresponding to a different bottom slope in the lateral y direction. The NS index for all data series is shown in Table 3.

The *DCM* results are always worse and are particularly bad for all the K series. The results of both the *IDCM* and *INCM* methods are very good for the two F series not used for calibration, but are both poor for the K series. The *LHRM* method is always the best and also performs very well in the K series. The reason is probably that the K series tests have very low discharges, and the constant $\alpha = 0.02$, the coefficient adopted in the *IDCM* method, does not fit the size of the subsections and Eq. (13) is not a good approximation of the mixing length α_H in Eq. (12) for low values of the water depth. In Figs. 3a and 3b the NS curves obtained by using *DCM*, *IDCM*, *INCM* and *LHRM*, for series F2 and K4, are shown.

4.2 Validation n.2 - Comparison with field data

Although rating curves are available in different river sites around the world, field validation of the uniform flow formulas is not easy, for at least two reasons:

1) The average friction factor f and the related Manning's coefficient are not known as in the lab case and the results of all the formulas need to be scaled according to the Manning's coefficient to be compared with the actually measured discharges;

2) River bed roughness does change, along with the Manning's coefficient, from one water stage to another (it usually increases along with the water level).

A possible way to circumvent the problem is to apply the compared methods in the context of a calibration problem, where both the average Manning's coefficient and the discharge hydrograph are computed from the known level hydrographs measured in two different river cross sections (Perumal et al., 2007; Aricò et al., 2009). The authors solved the diffusive wave simulation problem using one known level

394 hydrograph as the upstream boundary condition and the second one as the benchmark
395 downstream hydrograph for the Manning's coefficient calibration.
396 It is well-known in the parameter estimation theory (Aster et al., 2012) that the
397 uncertainty of the estimated parameters (in our case the roughness coefficient) grows
398 quickly with the number of parameters, even if the matching between the measured
399 and the estimated model variables (in our case the water stages in the downstream
400 section) improves. The use of only one single parameter over all the computational
401 domain is motivated by the need of getting a robust estimation of the Manning's
402 coefficient and of the corresponding discharge hydrograph.
403 Although the accuracy of the results is restricted by several modeling assumptions, a
404 positive indication about the robustness of the simulation model (and the embedded
405 relationship between the water depth and the uniform flow discharge) is given by: 1)
406 the match between the computed and the measured discharges in the upstream
407 section, 2) the compatibility of the estimated average Manning's coefficient with the
408 site environment.
409 The area of interest is located in the Alzette River basin (Gran-Duchy of
410 Luxembourg) between the gauged sections of Pfaffenthal and Lintgen (Fig. 4). The
411 river reach length is about 19 km, with a mean channel width of ~30 m and an
412 average depth of ~4 m. The river meanders in a relatively large and flat plain about
413 300 m, with a mean slope of ~0.08%.

414 The methodology was applied to a river reach 13 Km long, between two instrumented
415 sections, Pfaffenthal (upstream section) and Hunsdorf (downstream section), in order
416 to have no significant lateral inflow between the two sections.
417 Events of January 2003, January 2007 and January 2011 were analysed. For these
418 events, stage records and reliable rating curves are available at the two gauging
419 stations of Pfaffenthal and Hunsdorf. The main hydraulic characteristics of these
420 events, that is duration (Δt), peak water depth (H_{peak}) and peak discharge (q_{peak}), are
421 shown in Table 4.
422 In this area a topographical survey of 125 river cross sections was available. The
423 hydrometric data were recorded every 15 min. The performances of the discharge
424 estimation procedures were compared by means of the Nash Suctliffe criterion.
425 The results of the *INCM* and *LHRM* methods were also compared with those of the
426 *DCM* and *IDCM* methods, the latter applied by using α = 0.02 and an average

427 subsection width equal to 7 m. The computed average Manning's coefficients n_{opt},
428 reported in Table 5, are all consistent with the site environment, although they attain
429 very large values, according to *DCM* an *IDCM*, in the 2011 event.
430 The estimated and observed dimensionless water stages in the Hunsdorf gauged site,
431 for 2003, 2007 and 2011 events are shown in Figs. 5-7.
432 Only the steepest part of the rising limb, located inside the colored window of each
433 Figure, was used for calibration. The falling limb is not included, since it has a lower
434 slope and is less sensitive to the Manning's coefficient value.
435 A good match between recorded and simulated discharge hydrographs can be
436 observed (Figs. 8-10) in the upstream gauged site for each event.
437 For all investigated events the Nash Sutcliffe efficiency NS_q is greater than 0.90, as
438 shown in Table 6.
439 The error obtained between measured and computed discharges, with all methods, is
440 of the same order of the discharge measurement error. Moreover, this measurement
441 error is well known to be much larger around the peak flow, where the estimation
442 error has a larger impact on the NS coefficient. The NS coefficients computed with
443 the *LHRM* and *INCM* methods are anyway a little better than the other two.

444 *4.3 Validation n.3 - Comparison with results of 3D ANSYS CFX solver*

445 The vertically averaged velocities computed using *DCM*, *IDCM*, *INCM* and *LHRM*
446 were compared with the results of the well known ANSYS 3D code, named CFX,
447 applied to a prismatic reach with the irregular cross-section measured at the Hunsdorf
448 gauged section of the Alzette river. The length of the reach is about four times the top
449 width of the section.
450 In the homogeneous multiphase model adopted by CFX, water and air are assumed to
451 share the same dynamic fields of pressure, velocity and turbulence and water is
452 assumed to be incompressible. CFX solves the conservation of mass and momentum
453 equations, coupled with the air pressure-density relationship and the global continuity
454 equation in each node. Call α_l, ρ_l, μ_l and $\mathbf{U}_l$ respectively the volume fraction, the
455 density, the viscosity and the time averaged value of the velocity vector for phase l (l
456 = w (water), a (air)), that is:

457 $$\rho = \sum_{l=w,a} \alpha_l \rho_l \qquad (22a),$$

458 $$\mu = \sum_{l=w,a} \alpha_l \mu_l \quad (22b),$$

459 where ρ and μ are the density and the viscosity of the "averaged" phase. The air
460 density is assumed to be a function of the pressure *p*, according to the state equation:

461 $$\rho_a = \rho_{a,0} e^{\gamma(p-p_o)} \quad (22c),$$

462 where the sub-index 0 marks the reference state values and γ is the air compressibility
463 coefficient.
464 The governing equations are the following: 1) the mass conservation equation, 2) the
465 Reynolds averaged continuity equation of each phase and 3) the Reynolds averaged
466 momentum equations. Mass conservation implies:

467 $$\sum_{l=w,a} \alpha_l = 1 \quad (23).$$

468 The Reynolds averaged continuity equation of each phase *l* can be written as:

469 $$\frac{\partial \rho_l}{\partial t} + \nabla \cdot (\rho_l \, \mathbf{U}) = S_l \quad (24),$$

470 where S_l is an external source term. The momentum equation instead refers to the
471 "averaged" phase and is written as:

472 $$\frac{\partial (\rho \mathbf{U})}{\partial t} + \nabla \cdot (\rho \mathbf{U} \otimes \mathbf{U}) - \nabla \cdot \left(\mu_{eff} \left(\nabla \mathbf{U} + (\nabla \mathbf{U})^T \right) \right) + \nabla p' = S_M \quad (25),$$

473 where $\otimes$ is the dyadic symbol, S_M is the momentum of the external source term *S*, and
474 μ_{eff} is the effective viscosity accounting for turbulence and defined as:

475 $$\mu_{eff} = \mu + \mu_t \quad (26),$$

476 where μ_t is the turbulence viscosity and p' is the modified pressure, equal to:

477 $$p' = p + \frac{2}{3} \rho k + \frac{2}{3} \mu_{eff} \nabla \cdot \mathbf{U} \quad (27),$$

478 where *k* is the turbulence kinetic energy, defined as the variance of the velocity
479 fluctuations and *p* is the pressure. Both phases share the same pressure *p* and the same
480 velocity $\mathbf{U}$.
481 To close the set of six scalar equations (Eq.23, Eq.24 (two) and Eq.25 (three)), we
482 finally apply the *k*-ε turbulence model implemented in the CFX solver. The

implemented turbulence model is a two equation model, including two extra transport equations to represent the turbulent properties of the flow.

Two-equation models account for history effects like convection and diffusion of turbulent energy. The first transported variable is turbulent kinetic energy, k; the second transported variable is the turbulent dissipation, ε. The K-epsilon model has been shown (Jones, 1972; Launder, 1974) to be useful for free-shear layer flows with relatively small pressure gradients. Similarly, for wall-bounded and internal flows, the model gives good results, but only in cases where the mean pressure gradients are small.

The computational domain was divided using both tetrahedral and prismatic elements (Fig. 11). The prismatic elements were used to discretize the computational domain in the near-wall region over the river bottom and the boundary surfaces, where a boundary layer is present, while the tetrahedral elements were used to discretize the remaining domain. The number of elements and nodes, in the mesh used for the specific case are of the order respectively $4*10^6$ and $20*10^6$.

A section of the mesh is shown in Fig.12. The quality of the mesh was verified by using a pre-processing procedure by ANSYS® ICEM CFD™ (Ansys inc., 2006).

The six unknowns in each node are the pressure, the velocity components, and the volume fractions of the two phases. At each boundary node three of the first four unknowns have to be specified. In the inlet section a constant velocity, normal to the section, is applied, and the pressure is left unknown. In the outlet section the hydrostatic distribution is given, the velocity is assumed to be still normal to the section and its norm is left unknown. All boundary conditions are reported in Table 7.

The opening condition means that that velocity direction is set normal to the surface, but its norm is left unknown and a negative (entering) flux of both air and water is allowed. Along open boundaries the water volume fraction is set equal to zero. The solution of the problem converges towards two extremes: nodes with zero water fraction, above the water level, and nodes with zero air fraction below the water level.

On the bottom boundary, between the nodes with zero velocity and the turbulent flow a boundary layer exists that would require the modelling of micro scale irregularities. CFX allows the use, inside the boundary layer, of a velocity logarithmic law, according to an equivalent granular size. The relationship between the granular size and the Manning's coefficient, according to Yen (1994), is given by:

516 $$d_{50} = \left(\frac{n}{0.0474}\right)^6 \quad (28),$$

517 where d_{50} is the average granular size to be given as the input in the CFX code.
518 Observe that the assumption of known and constant velocity directions in the inlet and
519 outlet section is a simplification of reality. A more appropriate boundary condition at
520 the outlet section, not available in the CFX code, would have been given by zero
521 velocity and turbulence gradients (Rameshwaran et al. 2013). For this reason, a better
522 reconstruction of the velocity field can be found in an intermediate section, where
523 secondary currents with velocity components normal to the mean flow direction can
524 be easily detected (Peters and Goldberg, 1989; Richardson and Colin, 1996). See in
525 Fig. 13 how the intermediate section was divided to compute the vertically averaged
526 velocities in each segment section and, in Fig.14, the velocity components tangent to
527 the cross section plane.
528 These 3D numerical simulations confirm that the momentum Γ, proportional to the
529 derivative of the average tangent velocities and equivalent to the left hand side of Eq.
530 2, cannot be set equal to zero, if a rigorous reconstruction of the velocity field is
531 sought after.
532 To compute the uniform flow discharge, for a given outlet section, CFX code is run
533 iteratively, each time with a different average longitudinal velocity in the inlet section,
534 until the same water depth as in the outlet section is attained in the inlet section for
535 steady state conditions.Using the velocity distribution computed in the middle section
536 along the steady state computation as upstream boundary condition, transient analysis
537 is carried on until pressure and velocity oscillations become periodic.
538 In order to test the achievement of the fully developed state within the first half of the
539 modeled length the authors plotted the vertical profiles of the streamwise velocity
540 components for ten verticals, equally spaced along the longitudinal axis of the main
541 channel. See in Fig.15 the plot of four of them and their location. The streamwise
542 velocity evolves longitudinally and becomes almost completely self similar starting
543 from the vertical line in the middle section.
544 Stability of the results has been finally checked against the variation of the length of
545 the simulated channel. The dimensionless sensitivity of the discharge with respect to
546 the channel length is equal to 0.2%.

See in Table 8 the comparison between the vertically averaged state velocities, computed through the *DCM*, *IDCM*, *INCM*, *LHRM* formulas (u_{DCM}, u_{IDCM}, u_{INCM}, u_{LHRM}) and through the CFX code (u_{CFX}). Table 9 also shows the relative difference, Δu, evaluated as:

$$\Delta u = \frac{u - u_{CFX}}{u_{CFX}} \times 100 \quad (29),$$

As shown in Table 8, both *INCM* and *LHRM* perform very well in this validation test instead of *DCM*, which clearly overestimates averaged velocities. In the central area of the section the averaged velocities calculated by the *INCM*, *LHRM* and CFX code are quite close with a maximum difference ~7%. By contrast, larger differences are evident close to the river bank, in segments 1 and 9, where *INCM* and *LHRM* underestimate the CFX values. These larger differences show the limit of using a 1D code. Close to the bank the wall resistance is stronger and the velocity field is more sensitive to the turbulent exchange of energy with the central area of the section, where higher kinetic energy occurs. Thanks to the simulation of secondary flows (see Fig. 14) CFX allows this exchange and the related mixing. However, because the near-bank subsections are characterised by small velocities, their contribution to the global discharge and bed load is relatively small.

5 Conclusions

Two new methods computing the vertically averaged velocities along irregular sections have been presented. The first method, named *INCM*, develops from the original *IDCM* method and it is shown to perform better than the previous one, with the exception of lab tests with very small discharge values. The second one, named *LHRM*, has empirical bases, and gives up the ambition of estimating turbulent stresses, but has the following important advantages:

1. It relies on the use of only two parameters: the friction factor f (or the corresponding Manning's coefficient n) and a second parameter β which on the basis of the available laboratory data was estimated to be equal to 9.
2. The β coefficient has a simple and clear physical meaning: the correlation distance, measured in water depth units, of the vertically averaged velocities between two different verticals of the river cross-section.

577 3. The sensitivity of the results with respect to the model β parameter was shown to
578 be very low, and a one digit approximation is sufficient to get a discharge variability
579 less than 2%. A fully positive validation of the method was carried out using lab
580 experimental data, as well as field discharge and roughness data obtained by using
581 the unsteady-state level analysis proposed by Aricò et al. (Aricò et al., 2009) and
582 applied to the Alzette river, in the grand Duchy of Luxembourg.
583 4. Comparison between the results of the CFX 3D turbulence model and the *LHRM*
584 model shows a very good match between the two computed total discharges, although
585 the vertically averaged velocities computed by the two models are quite different near
586 to the banks of the river.
587 Moreover, it is well-known that bed load transport is directly related to the bed shear
588 stress and that this is proportional in each point of the section to the second power of
589 the vertically averaged velocity, according to Darcy Weisbach formula (Ferguson,
590 2007):

591 $$\tau_0 = \rho U^2 \frac{f}{8} \quad (30),$$

592 All the bed load formulas available in literature compute the solid flux per unit width.
593 For example, the popular Schoklisch formula (Gyr et al., 2006) is:

594 $$q_s = \frac{2.5}{\rho_s / \rho} S^{\frac{3}{2}} (q - q_c) \quad (31),$$

595 where q and q_s are respectively the liquid and the solid discharge per unit width. This
596 implies that the information given by the mean velocity and by the cross section
597 geometry is not sufficient for a good estimation of the bed load in irregular sections. If
598 Eq.(31) holds, the error in the bed load estimation is proportional to the error in the
599 volumetric discharge, discussed in the previous sections.
600
601

602 **Acknowledgements**

603 The authors wish to express their gratitude to the Administration de la gestionde l'eau
604 of Grand-Duché de Luxembourg and the Centre de Recherche Public "Gabriel
605 Lippmann" for providing hydrometric and topographical data on Alzette River.
606

607 **Notation**

608 A_i = area of each subsection "i" of a compound channel

609 B = top width of compound channel

610 b = main channel width at bottom

611 f = friction factor

612 g = gravity acceleration

613 H = total depth of a compound channel

614 n_{mc} and n_{fp}= Manning's roughness coefficient for the main channel and floodplain,
615 respectively

616 P_i = wetted perimeter of each subsection "i" of a compound channel

617 Q_{meas}= measured discharge

618 R_i = hydraulic radius of each subsection "i" of a compound channel

619 S_0 = longitudinal channel bed slope

620 S_f = energy slope

621 τ = turbulent stress

622 ε = turbulent dissipation

623 ρ = fluid density

624 μ = fluid viscosity

625 α = *IDCM* interface coefficient

626 β = *LHRM* coefficient

627 ξ = *INCM* coefficient

628

629

630

631

632

633

634

635

636

637 **References**

638

639 Abril, J. B., and Knight, D. W. (2004). Stage-discharge prediction for rivers in flood
640 applying a depth-averaged model. *J. Hydraul. Res*., 42(6), 616–629.
641
642 Ansys Inc., Canonsburg. (2006). ANSYS CFX Reference guide.
643
644 Ackers, P. (1993). Flow formulae for straight two-stage channels. *J. Hydraul. Res.*,
645 31(4), 509–531.
646
647 Aricò, C. and Tucciarelli, T. (2007). A Marching in Space and Time (MAST) solver
648 of the shallow water equations. Part I: the 1D model. Advances in Water Resources,
649 30(5), 1236-1252.
650
651 Aricò, C., Nasello, C. and Tucciarelli, T. (2009). Using unsteady water level data to
652 estimate channel roughness and discharge hydrograph, *Advances in Water Resources*;
653 32(8), 1223-1240.
654
655 Aster, C., Borchers, B., Clifford, H. (2012). Parameter Estimation and Inverse
656 Problems. Elsevier, ISBN: 978-0-12-385048-5.
657
658 Bousmar, D., and Zech, Y. (1999). Momentum transfer for practical flow computation
659 in compound channels. *J. Hydraul. Eng.*; 696–706.
660
661 Cao, Z., Meng, J., Pender, G., & Wallis, S. (2006). Flow resistance and momentum
662 flux in compound open channels. *J. Hydraul. Eng.*; 1272–1282.
663
664 Chow, V. T. (1959). Open channel hydraulics. New York: McGraw-Hill.
665

666 Corato, G., Moramarco, T., and Tucciarelli, T. (2011). Discharge estimation
667 combining flow routing and occasional measurements of velocity, *Hydrol. Earth Syst.*
668 *Sci.*,15, pp. 2979-2994.
669
670 Dey, M., and Lambert, M. F. (2006). Discharge prediction in compound channels by
671 end depth method. *J. Hydraul. Res.,*44(6), 767–776.
672
673 Ferguson, R. (2007) Flow resistance equations for gravel and boulder-bed streams.
674 *Water resources research*, 43, W05427.
675
676 Gyr, A, and Hoyer k. (2006), Sediment Transport A geophysical Phenomenon,
677 Springer, 30-31.
678
679 Herschel, C. (1897). On the origin of the Chezy formula, *J. Assoc. of Engineering*
680 *Soc.* 18, 363-368.
681
682 Hu, C., Ji, Z., and Guo, Q. (2010). Flow movement and sediment transport in
683 compound channels. *J. Hydraul. Res*., 48(1), 23–32.
684
685 Huthoff, F., Roos, P. C., Augustijn, D. C. M., and Hulscher, S. J. M. H. (2008).
686 Interacting divided channel method for compound channel flow. *J. Hydraul. Eng*.,
687 1158–1165.
688
689 Jones, W. P., and Launder, B. E. (1972). The Prediction of Laminarization with a
690 Two-Equation Model of Turbulence*, International Journal of Heat and Mass*
691 *Transfer*; vol. 15, pp. 301-314.
692
693 Kejun Yang, Xingnian Liu; ShuyouCao and Er Huang. (2013). Stage-Discharge
694 Prediction in Compound Channels, *J. Hydraul. Eng.*
695
696 Knight, D. W., and Abril, B. (1996).Refined calibration of a depth averaged model for
697 turbulent flow in a compound channel. *Proc. ICE Water Maritime Energy*; 118(3),
698 151–159.
699

700 Knight, D.W., and Demetriou, J. D. (1983). Flood plain and main channel flow
701 interaction, *J. Hydraul. Eng.*, 1073–1092.
702
703 Knight, D. W., and Hamed, M. E. (1984).Boundary shear in symmetrical compound
704 channels, *J. Hydraul. Eng.*, 1412–1430.
705
706 Knight, D. W., McGahey, C., Lamb, R., and Samuels, P. G. (2010).Practical channel
707 hydraulics: Roughness, conveyance and afflux. CRC Press/Taylor and Francis,
708 Leiden, The Netherlands, 1–354.
709
710 Knight, D. W., and Sellin, R. H. J. (1987). The SERC flood channel facility. *J. Inst.*
711 *Water Environ.* Manage, 1(2), 198–204.
712
713 Knight, D. W., and Shiono, K. (1996). River channel and floodplain hydraulics.
714 Chapter 5, Floodplain processes, M. G. Anderson,D. E. Walling, and P. D. Bates,
715 eds., Wiley, New York, 139–181.
716
717 Knight, D. W., Shiono, K., and Pirt, J. (1989).Prediction of depth mean velocity and
718 discharge in natural rivers with overbank flow. Proc., Int. Conf. on Hydraulic and
719 Environmental Modelling of Coastal, Estuarine and River Waters, R. A. Falconer, P.
720 Goodwin and R. G. S. Matthew, eds., Gower Technical, Univ. of Bradford, U.K.,
721 419–428.
722
723 Lambert, M. F., and Sellin, R. H. J. (1996). Discharge prediction in straight
724 compound channels using the mixing length concept. *J.Hydraul. Res.*,34(3), 381–394.
725
726 Launder, B. E., and Sharma, B. I. (1974). Application of the Energy Dissipation
727 Model of Turbulence to the Calculation of Flow Near a Spinning Disc. Letters in Heat
728 and Mass Transfer; vol. 1, no. 2, pp. 131-138.
729
730 Liao, H., and Knight, D. W. (2007). Analytic stage-discharge formulas for flow in
731 straight prismatic channels. *J. Hydraul. Eng.*, 1111–1122.
732

733 Lyness, J. F., Myers, W. R. C., Cassells, J. B. C., and O'Sullivan, J. J. (2001). The
734 influence of planform on flow resistance in mobile bed compound channels *Proc.,*
735 *ICE Water Maritime Eng.*; 148(1), 5–14.
736
737 McGahey, C. (2006). A practical approach to estimating the flow capacity of rivers.
738 Ph.D. thesis, The Open Univ., Milton Keynes, U.K,. (British Library).
739
740 McGahey, C., Knight, D. W., and Samuels, P. G. (2009). Advice, methods and tools
741 for estimating channel roughness. *Proc. ICE Water Manage,* 162(6), 353–362.
742
743 Moreta, P. J. M., and Martin-Vide, J. P. (2010). Apparent friction coefficient in
744 straight compound channels. *J. Hydraul. Res.*, 48(2), 169–177.
745
746 Myers,W. R. C., & Brennan, E. K. (1990). Flow resistance in compound channels. *J.*
747 *Hydraul. Res.*, 28(2), 141–155.
748
749 Omran, M., and Knight, D. W. (2010). Modelling secondary cells and sediment
750 transport in rectangular channels. *J. Hydraul. Res.*, 48(2), 205–212.
751
752 Peters J.J. and Goldberg A. (1989). Flow data in large alluvial channels in
753 Maksimovic, C. &Radojkovic, M. (eds) Computational Modeling and Experimental
754 methods in Hydraulics; Elsevier, London, 77-86.
755

756 Perumal M, Moramarco T, Sahoo B, Barbetta S. (2007). A methodology for discharge
757 estimation and rating curve development at ungauged river sites. *Water Resources*
758 *Res.*
759
760 Rameshwaran, P. and Shiono, K. (2007). Quasi two-dimensional model for straight
761 overbank flows through emergent vegetation on floodplains. . *J. Hydraul. Res. 45(3),*
762 *302-315.*
763
764 Rameshwaran, Ponnambalam; Naden, Pamela; Wilson, Catherine A.M.E.; Malki,
765 Rami; Shukla, Deepak R.; Shiono, Koji. (2013). Inter-comparison and validation of

766 computational fluid dynamics codes in two-stage meandering channel flows. *Applied*
767 *Mathematical Modelling*, 37 (20-21). 8652-8672.
768
769 Rhodes, D. G., and Knight, D. W. (1994). Velocity and boundary shear in a wide
770 compound duct. *J. Hydraul. Res.,*32(5), 743–764.
771
772 Richardson R. W. and Colin R. Thorne. (1998). Secondary Currents around Braid Bar
773 inBrahmaputra River, Bangladesh. *J. Hydraul. Eng.*, 124(3), 325–328.
774
775 Schlichting, H. (1960). Boundary layer theory, 4th Ed., McGraw-Hill,NewYork.
776
777 Sellin, R. H. J. (1964). A laboratory investigation into the interaction between the
778 flow in the channel of a river and that over its flood plain. La Houille Blanche, 7,
779 793–801.
780
781 Shiono, K., Al-Romaih, J. S., and Knight, D. W. (1999). Stage-discharge assessment
782 in compound meandering channels. *J. Hydraul. Eng.*, 66–77.
783
784 Shiono, K., and Knight, D. W. (1991). Turbulent open-channel flows with variable
785 depth across the channel. *J. Fluid Mech.*,222, 617–646.
786
787 Stephenson, D., andKolovopoulos, P. (1990). Effects of momentum transfer in
788 compound channels. *J. Hydraul. Eng.*, 1512–1522.
789
790 Tang, X., and Knight, D. W. (2008). Lateral depth-averaged velocity distributions
791 and bed shear in rectangular compound channels. *J. Hydraul. Eng.*, 1337–1342.
792
793 Van Prooijen, B. C., Battjes, J. A., andUijttewaal, W. S. J. (2005). Momentum
794 exchange in straight uniform compound channel flow. *J. Hydraul. Eng.*, 175–183.
795
796 Wormleaton, P. R., Allen, J., andHadjipanos, P. (1982). Discharge assessment in
797 compound channel flow. *J. Hydraul. Div.*, 108(9), 975–994.
798

799 Wormleaton, P. R., &Hadjipanos, P. (1985). Flow distribution in compound channels.
800 *J. Hydraul. Eng.*, 357–361.
801
802 Yen, B.C. (1992).The Manning formula in context. Channel Flow Resistance:
803 Centennial of Manning's Formula,. Editor Water Resources Publications, Littleton,
804 Colorado, USA, p. 41.
805
806 MIKE11, A Modelling System for Rivers and Channels, Reference Manual, DHI
807 2009
808 HEC-RAS, River Analysis System, Hydraulic Reference Manual, US Army Corps of
809 Engineers 2010.
810

811 Table 1 Geometric and Hydraulic Laboratory Parameters of the experiment series.

Series	S_0 [‰]	h [m]	B [m]	b_4 [m]	b_1 [m]	b_3 [m]	s_{fp} [-]	s_{mc} [-]
F1	1.027	0.15	1.8	1.5	4.1	4.100	0	1
F2					2.25	2.250	1	1
F3					0.75	0.750	1	1
F6					2.25	0	1	1
F8					2.25	2.250	1	0
F10					2.25	2.250	1	2
K1	0.966	0.08	0.15	0.152	0.229	0.229	0	0
K2					0.152	0.152		
K3					0.076	0.076		
K4					-	-		

812

813 Table 2a Sensitivities I_s and L_s computed in the F2 series for the optimal parameter
814 values.

H [m]	Q_{meas}[m^3s^{-1}]	I_s	L_s
0.156	0.212	0.2209	0.2402
0.169	0.248	0.1817	0.2194
0.178	0.282	0.1651	0.2044
0.187	0.324	0.1506	0.1777
0.198	0.383	0.1441	0.1584
0.214	0.480	0.1305	0.1336
0.249	0.763	0.1267	0.1320

815

816 Table 2b Sensitivities I_s and L_s computed in the K4 series for the optimal parameter
817 values.

H [m]	Q_{meas} [m^3s^{-1}]	I_s	L_s
0.085	0.005	0.3248	0.3282
0.096	0.008	0.2052	0.2250
0.102	0.009	0.1600	0.1709
0.114	0.014	0.1354	0.1372

0.127	0.018	0.1174	0.1208
0.154	0.029	0.0851	0.0866

818

819 Table 3 Nash-Sutcliffe Efficiency for all (calibration and validation) experimental
820 series.

	Series	*DCM*	*IDCM*	*INCM*	*LHRM*
Calibration Set	*F1*	0.7428	0.9807	0.9847	0.9999
	F2	0.6182	0.9923	0.9955	0.9965
	F3	0.7219	0.9744	0.9261	0.9915
	F6	0.7366	0.9733	0.9888	0.9955
Validation Set	*F8*	-0.0786	0.9881	0.9885	0.9964
	F10	-0.0885	0.9965	0.9975	0.9978
	K1	-14.490	-0.7007	-8.2942	0.9968
	K2	-0.9801	0.3452	-1.8348	0.9619
	K3	0.1762	0.6479	-0.3944	0.9790
	K4	0.2878	0.888	0.3548	0.9958

821

822 Table 4 Main characteristics of the flood events at the Pfaffenthal and Hunsdorf
823 gauged sites.

Event	Δt [h]	Pfaffenthal		Hunsdorf	
		H_{peak} [m]	q_{peak} [m^3s^{-1}]	H_{peak} [m]	Q_{peak} [m^3s^{-1}]
January 2003	380	3.42	70.98	4.52	67.80
January 2007	140	2.90	53.68	4.06	57.17
January 2011	336	3.81	84.85	4.84	75.10

824

825

826

827

828

829

830

831 Table 5 Optimum roughness coefficient, n_{opt}, for the three flood events.

Event	*DCM* n_{opt} [$sm^{-1/3}$]	*IDCM* n_{opt} [$sm^{-1/3}$]	*INCM* n_{opt} [$sm^{-1/3}$]	*LHRM* n_{opt} [$sm^{-1/3}$]
January 2003	0.054	0.047	0.045	0.045
January 2007	0.051	0.047	0.046	0.045
January 2011	0.070	0.070	0.057	0.055

832

833 Table 6 Nash-Sutcliffe efficiency of estimated discharge hydrographs for the analysed
834 flood events.

Event	*DCM* NS_q [-]	*IDCM* NS_q [-]	*INCM* NS_q [-]	*LHRM* NS_q [-]
January 2003	0.977	0.987	0.991	0.989
January 2007	0.983	0.988	0.989	0.992
January 2011	0.898	0.899	0.927	0.930

835

836 Table 7 Boundary conditions assigned in the CFX simulation.

837

Geometry Face	Boundary Condition
Inlet	All velocity components
Outlet	Velocity direction and hydrostatic pressure distribution
Side-Walls	Opening
Top	Opening
Bottom	No-slip wall condition, with roughness given by equivalent granular size d_{50}.

838

839

840

841

842

843

844

845

846

847 Table 8 Simulated mean velocities in each segment section using 1D hydraulic
848 models with *DCM*, *IDCM*, *INCM*, *LHRM* and *CFX*, and corresponding differences.

Subsection	u_{CFX} [ms^{-1}]	u_{DCM} [ms^{-1}]	u_{IDCM} [ms^{-1}]	u_{INCM} [ms^{-1}]	u_{LHRM} [ms^{-1}]	Δu_{DCM} [%]	Δu_{IDCM} [%]	Δu_{INCM} [%]	Δu_{LHRM} [%]
1	1.33	1.58	1.47	1.23	1.12	18.79	10.52	-7.52	-15.78
2	1.37	1.42	1.4	1.36	1.38	3.65	2.19	-0.73	0.73
3	1.38	1.53	1.48	1.38	1.4	10.87	7.25	0	1.45
4	1.47	1.64	1.6	1.56	1.57	11.56	8.84	6.13	6.80
5	1.53	1.94	1.8	1.59	1.61	26.79	17.65	3.92	5.23
6	1.57	2.01	1.81	1.6	1.68	28.02	15.29	1.91	7.00
7	1.46	1.66	1.65	1.49	1.5	13.69	13.01	2.05	2.74
8	1.42	1.48	1.46	1.44	1.43	4.22	2.82	1.40	0.70
9	0.88	0.91	0.90	0.70	0.69	3.40	2.27	-20.45	-21.59

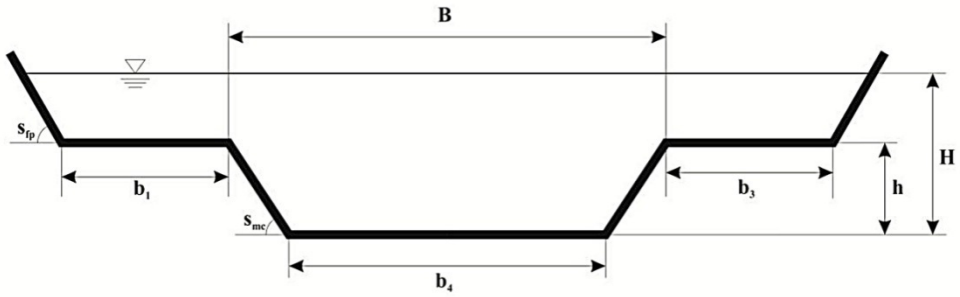

849

850 Figure 1 Compound channel geometric parameters.

851

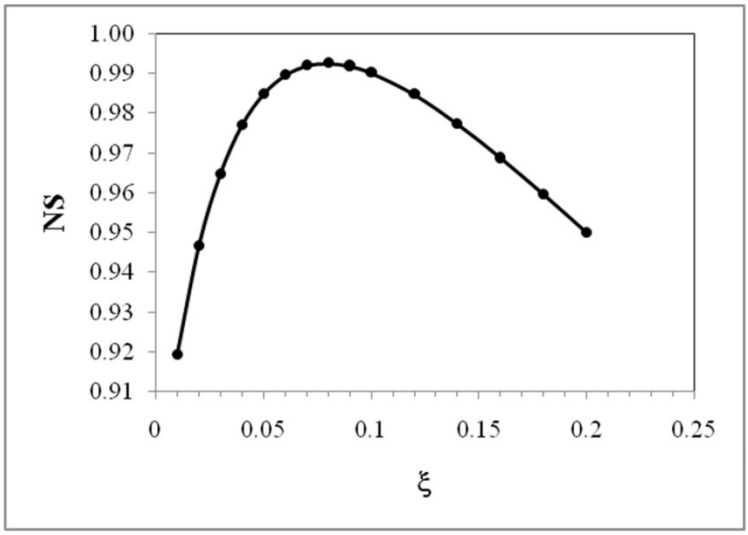

a)

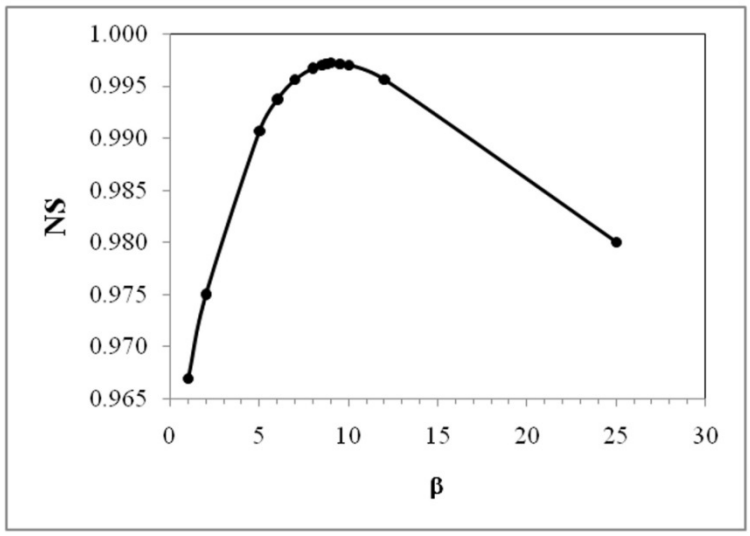

b)

Figure 2 NS versus ξ and β curves respectively for *INCM* (a) and *LHRM* (b) methods.

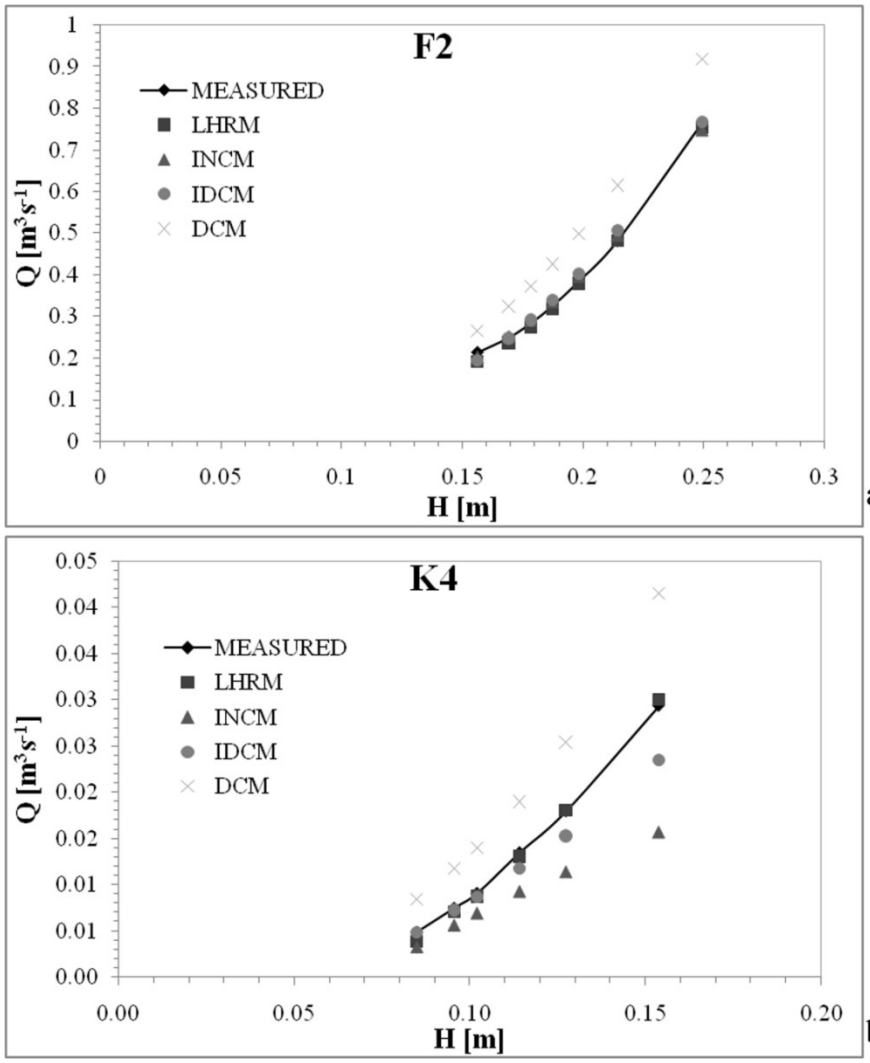

855

856 Figure 3 Estimated discharge values against HR Wallingford FCF measures for F2 (a)
857 and K4 (b) series.

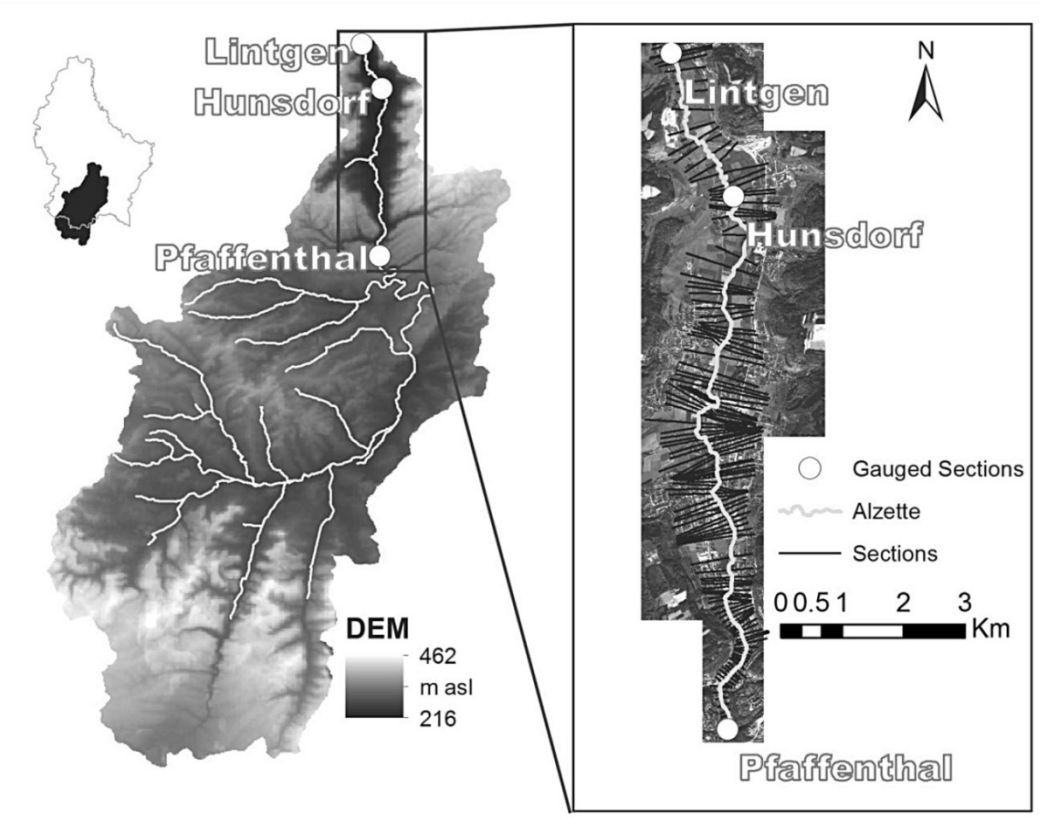

858

859 Figure 4 The Alzette Study Area.

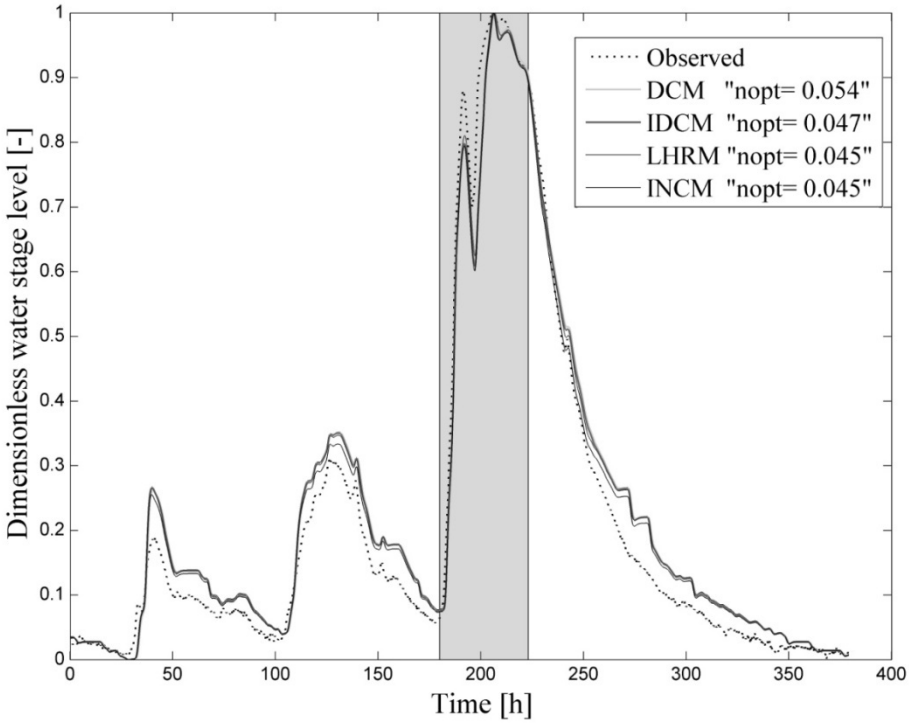

860

861 Figure 5 Observed and simulated stage hydrographs at Hunsdorf gauged site in the
862 event of January 2003.

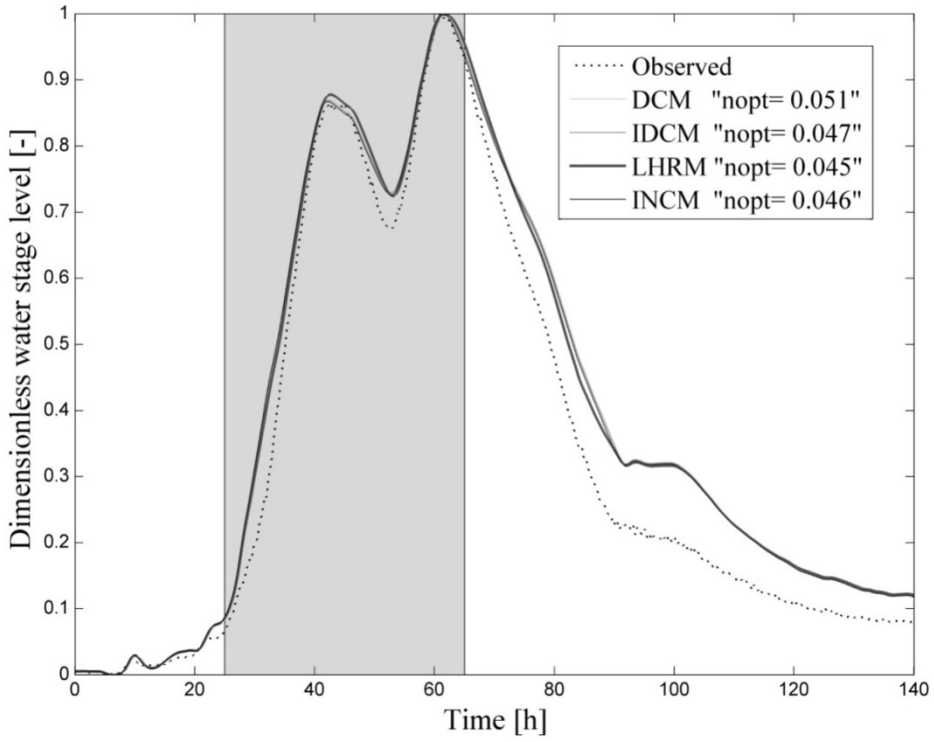

863

864 Figure 6 Observed and simulated stage hydrographs at Hunsdorf gauged site in the
865 event of January 2007.

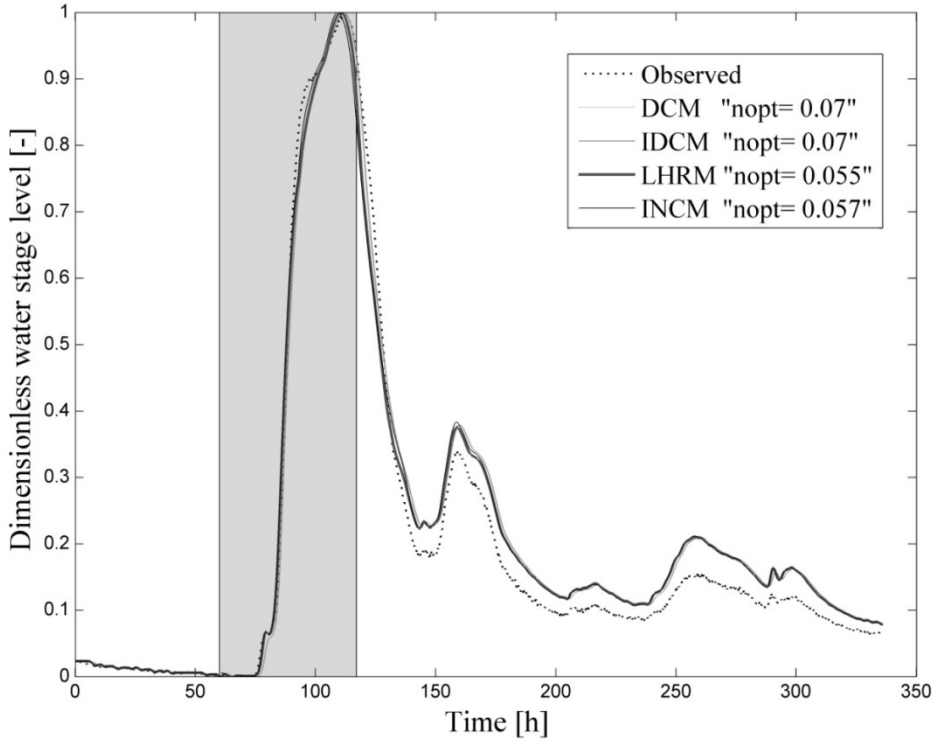

866

867 Figure 7 Observed and simulated stage hydrographs at Hunsdorf gauged site in the
868 event of January 2011.

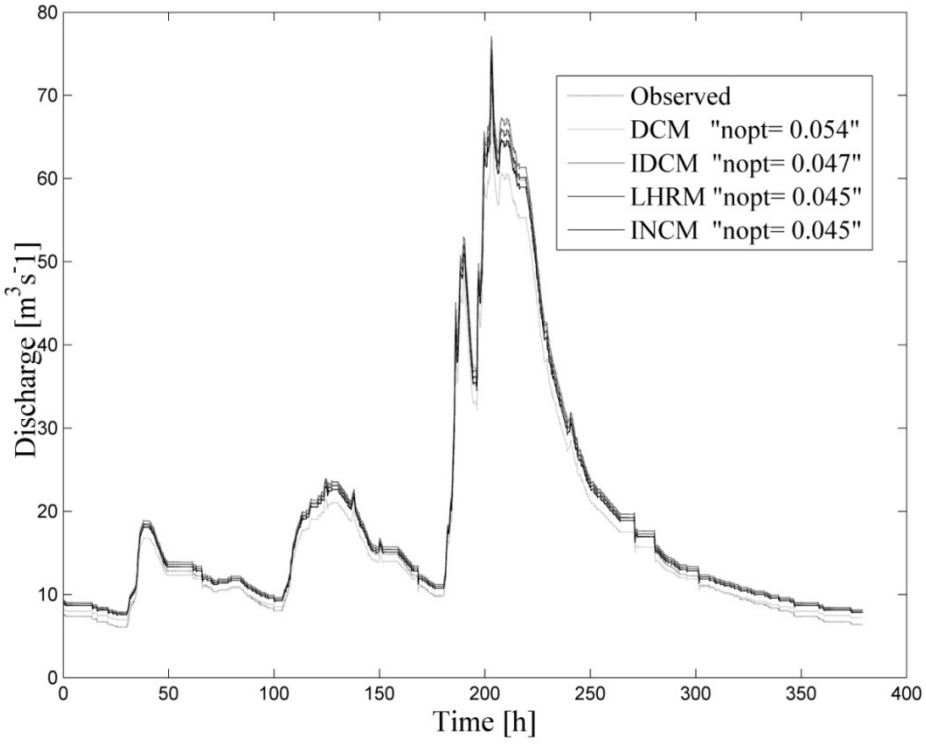

869

870 Figure 8 Observed and simulated discharge hydrographs at Pfaffenthal gauged site in
871 the event of January 2003.

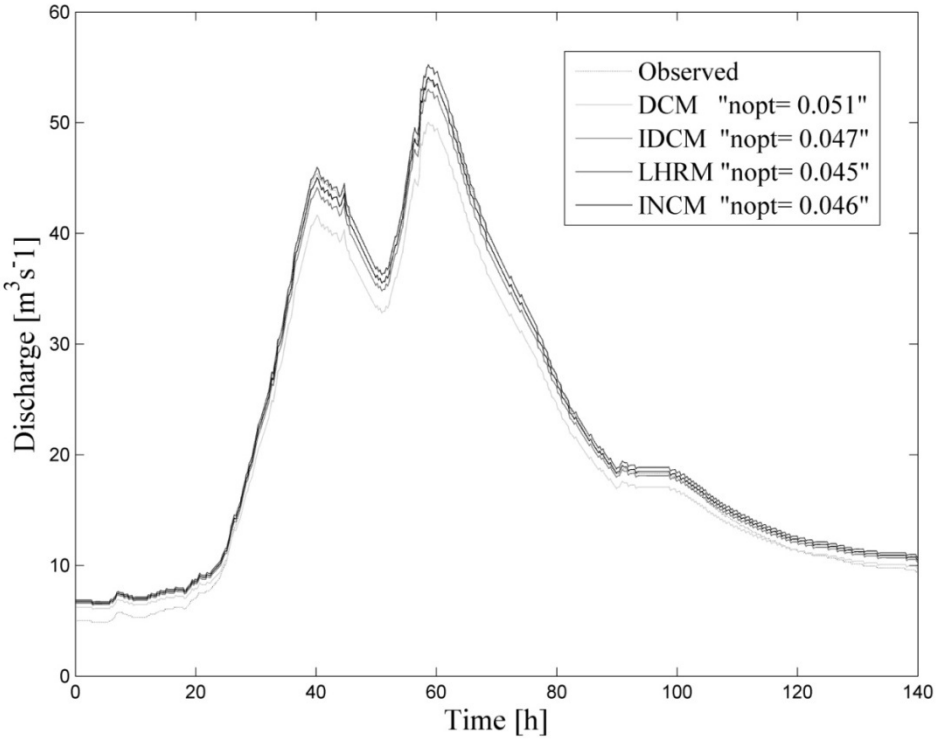

872

873 Figure 9 Observed and simulated discharge hydrographs at Pfaffenthal gauged site in
874 the event of January 2007.

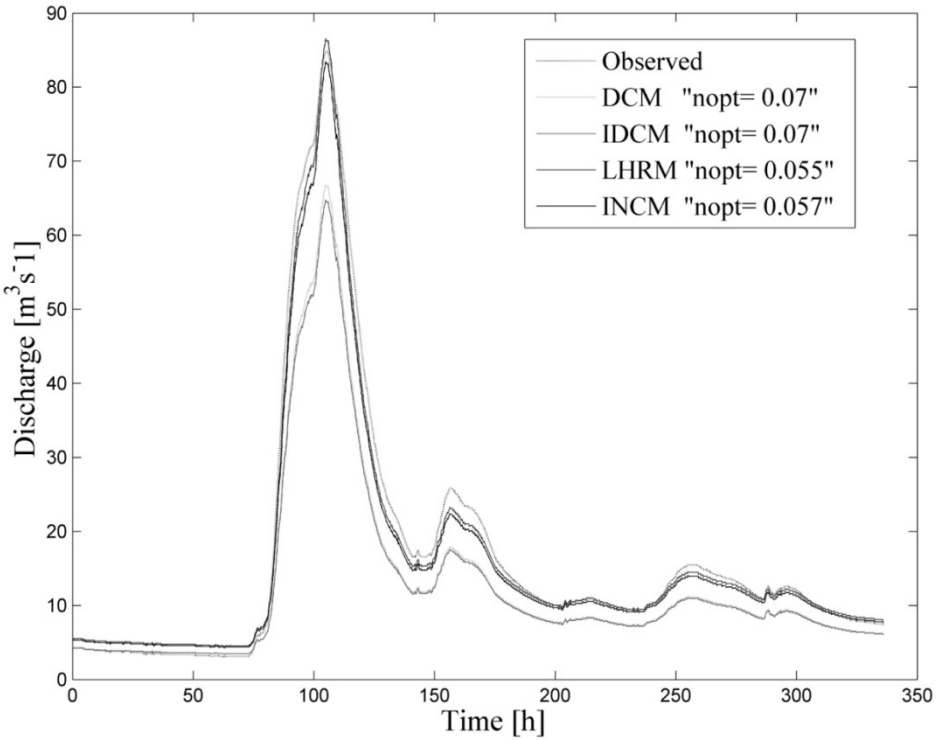

875

876 Figure 10 Observed and simulated discharge hydrographs at Pfaffenthal gauged site in
877 the event of January 2011.

878

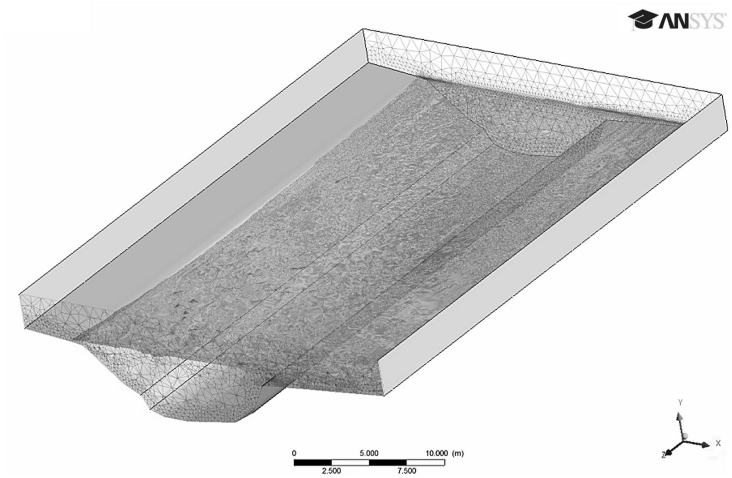

879

880 Figure 11 Computational domain of the reach of the Alzette river.

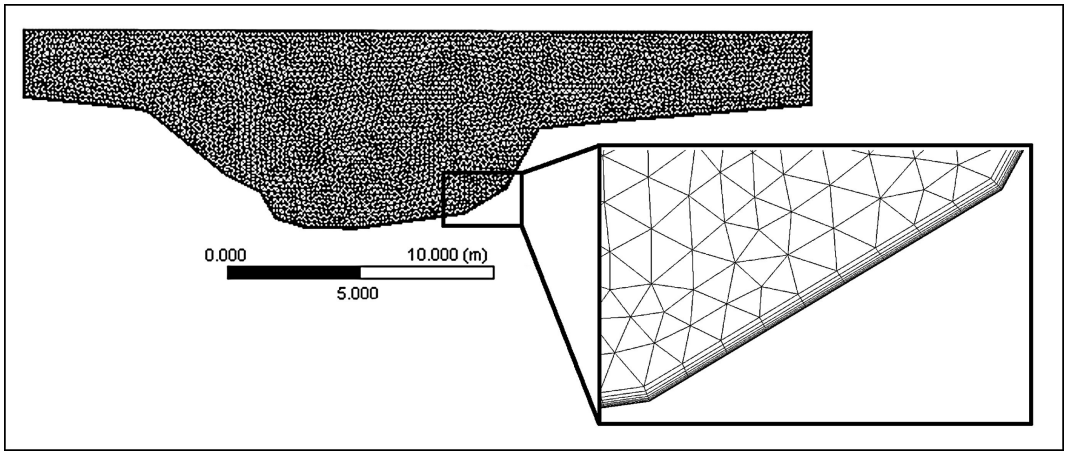

881

882 Figure 12 A mesh section along the inlet surface.

883

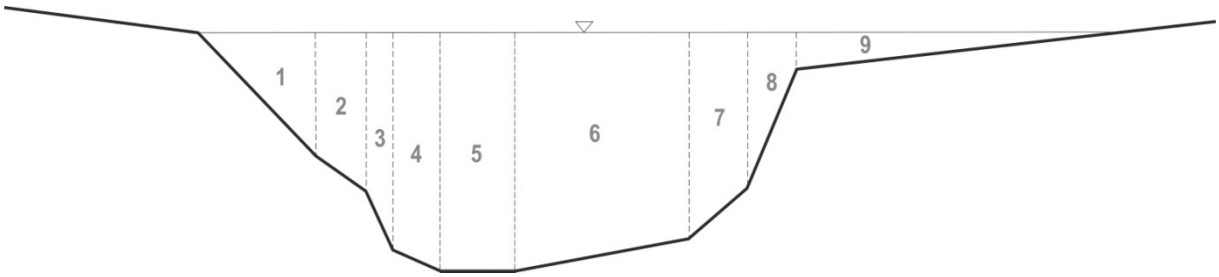

884

885 Figure 13 Hunsdorf river cross-section: subsections used to compute the vertically
886 averaged velocities.

887

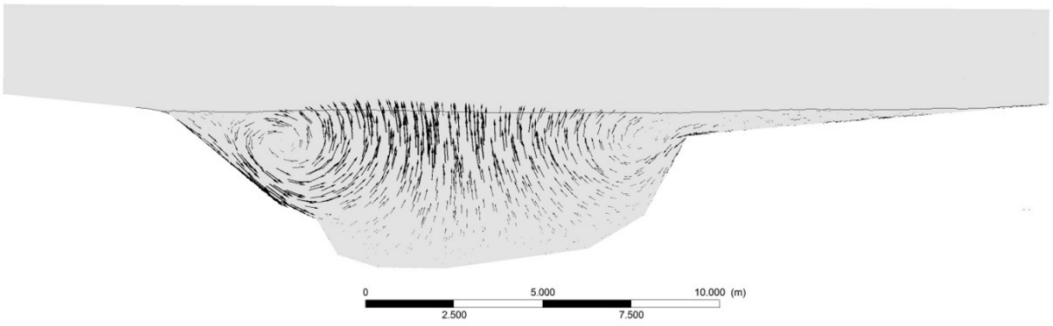

888

889 Figure 14 Secondary flow inside the intermediate cross section.

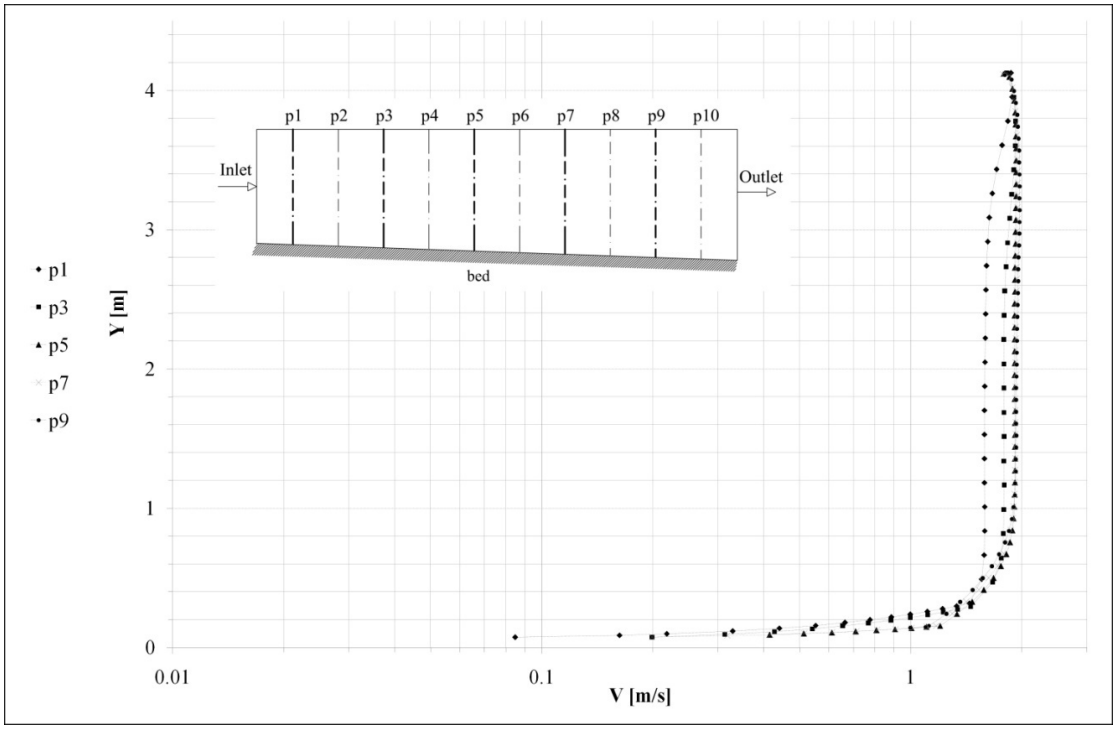

Figure 15 Streamwise vertical profile along the longitudinal axis of the mean channel.